Dalton Transactions

Accepted Manuscript

ROYAL SOCIETY OF CHEMISTRY

www.rsc.org/dalton

Mechanism of Catalytic Methylation of 2-Phenylpyridine Using di-*tert*-Butyl Peroxide

Akhilesh K. Sharma, Dipankar Roy, and Raghavan B. Sunoj*

Department of Chemistry
Indian Institute of Technology Bombay
Mumbai 400076,
Fax: (+91) 22-2576-7152
E-mail: sunoj@chem.iitb.ac.in

Abstract

The mechanism of palladium chloride-catalyzed direct methylation of arenes with peroxides is elucidated by using the energetics computed at the M06 density functional theory. The introduction of a methyl group by *tert*-butyl peroxides at the *ortho*-position of a prototypical 2-phenyl pyridine, a commonly used substrate in directed C–H functionalization reactions, is examined in detail by identifying the key intermediates and transition states involved in the reaction sequence. Different possibilities differing in terms of the site of catalyst coordination with the substrate and the ensuing mechanism are presented. The important mechanistic events involved are (a) an oxidative or a homolytic cleavage of the peroxide O–O bond, (b) C–H bond activation, (c) C–C bond activation, and (d) reductive elimination involving methyl transfer to the aromatic ring. We have examined both radical and non-radical pathways. In the non-radical pathway, the lowest energy pathway involves C–H bond activation prior to the coordination of the peroxide to palladium, which is subsequently followed by the O–O bond cleavage of the peroxide. Reductive elimination in the resultant intermediate leads to the vital C–C bond formation between methyl and aryl carbon atoms. In the non-radical pathway, the C–C bond activation is higher in energy and is identified as the rate-limiting step of this reaction. In radical pathway, however, the activation barrier for the C–C bond cleavage is lower than for the peroxide O–O bond cleavage. A combination of radical pathway up to the formation of a palladium methyl intermediate and a subsequent non-radical pathway is identified as the most favored pathway for the title reaction. The predicted mechanism is in good agreement with the experimental observations on PdCl2 catalyzed methylation of 2-phenyl pyridine using *tert*-butyl peroxide.

Introduction

The palladium catalyzed activation of aryl C–X bond (where X = hydrogen, halides, and sulfur) and the subsequent formation of Pd–C bond constitute the initiation step in several synthetically important reactions.[1] Amongst the plethora of examples on palladium-catalyzed reactions, the most widely reported ones include the activation of a carbon-halogen bond, such as in a coupling reaction.[2] The activation of a C–H bond followed by a C–C bond formation is effectively utilized in transition-metal-catalyzed coupling reactions.[3] In addition to palladium, other transition metals such as ruthenium and rhodium are extensively employed toward achieving catalyzed carbo-functionalization of arenes.[4] Some of the quintessential examples for arene functionalization employing Pd-catalysts are Suzuki,[5] Heck,[6] and Corriu-Kumada[7] coupling reactions.[8] The nature of the substrate and the catalyst can exert a direct influence on the mechanistic features as well as on the outcome of such reactions. The kinetic and mechanistic investigations on important coupling reactions have remained the subject of recent investigations.[9] There have been several interesting computational studies toward understanding C-H bond activation as well as coupling reactions.[10]

Alkylation of arenes through C–H activation using electrophilic transition metal catalysts is another widely pursued area of research.[11] The activation of olefinic, allylic as well as alkynyl C–H bonds and further chemical transformations has been achieved using Pd(II)-catalysts.[12] Among the myriad of applications of palladium-catalyzed reactions, the *ortho*-alkylation and *ortho*-arylation of arenes are of additional interest, owing to their importance toward the synthesis of biaryls as well as substituted aryls.[13] In a recent study, Li and co-workers have reported a novel Pd(II)-catalyzed methylation of arenes by using peroxides, as shown in Scheme 1.[14b] The use of peroxide is proposed to serve as a methylating agent first and as a proton

acceptor later in the reaction sequence. Interestingly, in the absence of the Pd(II)-catalyst, the methylation reaction failed to take place.

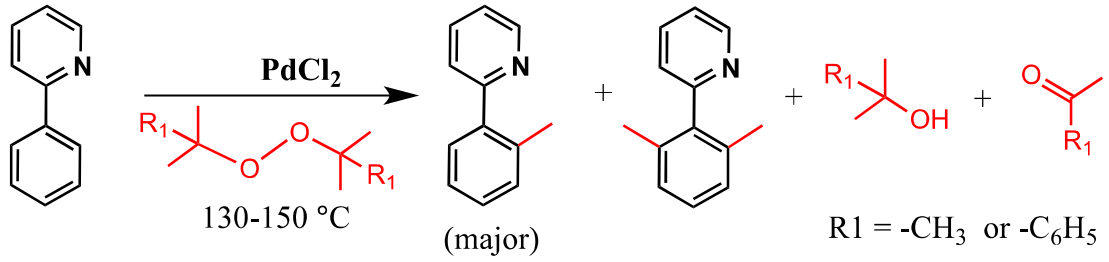

Scheme 1 $PdCl_2$-catalyzed methylation of 2-phenyl pyridine by di-*tert*-butyl peroxides.

The reaction can be broadly viewed as involving the following mechanistic events, consisting of four key elementary steps such as (i) the cleavage of the peroxide O–O linkage resulting in the formation of a Pd(IV) intermediate, (ii) the reductive methyl elimination facilitating the transfer of the methyl group to palladium,[15] (iii) the aryl C–H activation and palladation of the aryl ring, and (iv) lastly, the C–C coupling reaction to furnish the methylated arene. The involvement of higher oxidation state palladium(IV) intermediates is evident in this catalytic sequence.[16] While the qualitative mechanistic proposal appears to offer a reasonable rationalization of the experimental observations, several questions remain open. Although the qualitative mechanism is supported by the experiments of Li and coworkers,[13b] some of the pertinent observations demand more detailed mechanistic insights. The formation of a tertiary alcohol and a ketone has been found to be in near quantitative proportions.

The direct alkylation reactions are of high significance from a synthetic standpoint. The mechanistic insights would undoubtedly help exploit the potential of such reactions more effectively. In the present study, we intend to shed light on the mechanism of palladium-catalyzed direct methylation of 2-phenylpyridine as a prototypical arenes by using peroxides.

The approach includes detailed analysis of the structural and energetic features of the important intermediates and the transition states associated with each elementary step in the catalytic cycle.

Computational Methods

All calculations were carried out using Gaussian03 and Gaussian09 suite of quantum chemical programs.[17] The hybrid density functional mPW1K is used in conjunction with the LANL2DZ basis set consisting of effective core potential (ECP) for 28 electrons and Hay-Wadt's valance basis functions for all other electrons of palladium.[18,19] The remaining elements were represented using Pople's triple-zeta basis set consisting of polarization functions on hydrogen and non-hydrogen atoms along with a set of diffuse function, 6-311+G**. The choice of the mPW1K functional is primarily guided by the literature reports on its successful applications in the reactions involving organometallic compounds.[20] Energies were additionally refined by using the M06 functional on the mPW1K optimized geometries with the same basis sets.[21] The nature of the stationary points was first verified by the visual inspection of the imaginary frequencies pertaining to the desired reaction coordinate. The transition states were characterized by one and only one imaginary frequency representing the reaction coordinate. Further, the intrinsic reaction coordinate (IRC) analysis was performed to authenticate the crucial transition states.[22] The natural bond orbital (NBO) analysis was performed at the mPW1K/LANL2DZ, 6-311+G** level of theory.[23] The Gibbs free energies (ΔG_{298K}) and enthalpies (ΔH_{298K}) were calculated by using the standard statistical mechanical treatment (within the rigid rotor and harmonic oscillator approximations) wherein thermal and entropic corrections included. The results are presented on the basis of the energetics obtained at the M06/LANL2DZ(Pd),6-311+G**//mPW1K/LANL2DZ(Pd),6-311+G** level of theory.

The geometry optimization open-shell species with unpaired spin was performed using the UmPW1K/LANL2DZ(Pd),6-311+G** level of theory. The calculated $<S^2>$ values were in the range of 0.75–0.90 for doublets, and 2.01–2.12 for triplets respectively. The singlet biradical species were optimized using the initial orbital guess as obtained from the INDO method using the GUESS=(MIX,INDO) keyword.

Results and Discussion

The mechanistic features of palladium-catalyzed direct methylation of an aryl C–H bond of 2-phenylpyridine by *tert*-butyl peroxides are presented here. All the energy parameters such as the relative enthalpies and Gibbs free energies are reported with respect to the $PdCl_2$-substrate complex (**a**), unless specified otherwise. The experimental procedure involves the addition of catalyst palladium chloride to the reaction mixture containing both reactants, namely, *tert*-butyl peroxide and 2-phenylpyridine. Under such homogeneous reaction conditions, different sequence of combinations between the catalyst and the reactants could be envisaged. For instance, the catalyst could first combine either with 2-phenylpyridine or with the peroxide. A situation wherein both these reactants are bound to the catalyst prior to the generation of the active species could also be considered. Such likely coordination possibilities offer considerable challenges toward ascertaining the key active species in the catalytic cycle as well as in arriving at a convincing mechanistic picture. On the basis of the sequence of coordination and the ensuing catalytic action on the substrates, four key pathways are presented in this article. Although the qualitative mechanism initially proposed by Li and coworkers considers the coordination of the peroxide ahead of 2-phenylpyridine, we believe that a species like 2-phenylpyridine is likely to be more preferred by palladium(II) over the other weakly coordinating ligands.

The first pathway considered in this study involves the coordination of 2-phenylpyridine to $PdCl_2$ thereby facilitating an aryl C–H bond activation, followed by the reaction with the peroxide (pathway 1). In the second pathway, peroxide coordination and the cleavage of O–O bond is considered as occuring prior to the reaction with 2-phenylpyridine (pathway 2). The remaining two possibilities consist of simultaneous coordination of 2-phenylpyridine and peroxide to the catalyst. The latter two possibilities differing in the sequence of action of the catalyst on the substrates give rise to pathways 3 and 4. The discussion is broadly divided into four parts on the basis of these different pathways.

Pathway 1: Catalyst Coordination to 2-Phenylpyridine

In pathway 1, the complex Pd(II)-chloride-2-phenylpyridine (**a**) is considered as the starting point (Scheme 2). Improved proximity between the *ortho* C–H bond of the phenyl group and the coordinatively unsaturated palladium facilitates an effective agostic interaction in intermediate **a** (Fig. 1).[24] The ensuing C–H activation can lead to the formation of a cyclometallated species **b**.[25] The transition state for the C–H insertion **TS(a-b)** indicates a palladium mediated proton transfer from the aryl carbon to the chloride bound to the palladium center. The resulting square planar species **b** is identified as a minimum on the potential energy surface, and is of same energy as **a**. In **b**, one of the coordination sites of the palladium is occupied by a molecule of HCl. The Gibbs free energy barrier for the formation of **b** from **a** is 35 kcal/mol which involves the transfer of proton from the aryl ring to the chloride ligand. A two-step alternative route is also identified for the formation of intermediate **b**, wherein the transfer for the aryl proton occurs, first to the nearer chloride ligand. The activation barrier for this step is about 10 kcal/mol lower than that to the transfer to the farther chloride. However, the resulting

intermediate **b'** is higher in energy by 12.6 kcal/mol and lacks the intramolecular hydrogen bonding stabilization as compared to that in **b**. The conversion of **b'** to **b** is found to be quite facile with a very low activation barrier (0.4 kcal/mol). Hence, the conversion of intermediate **a** to **b** should be regarded as occuring in two steps through intermediate **b'**.

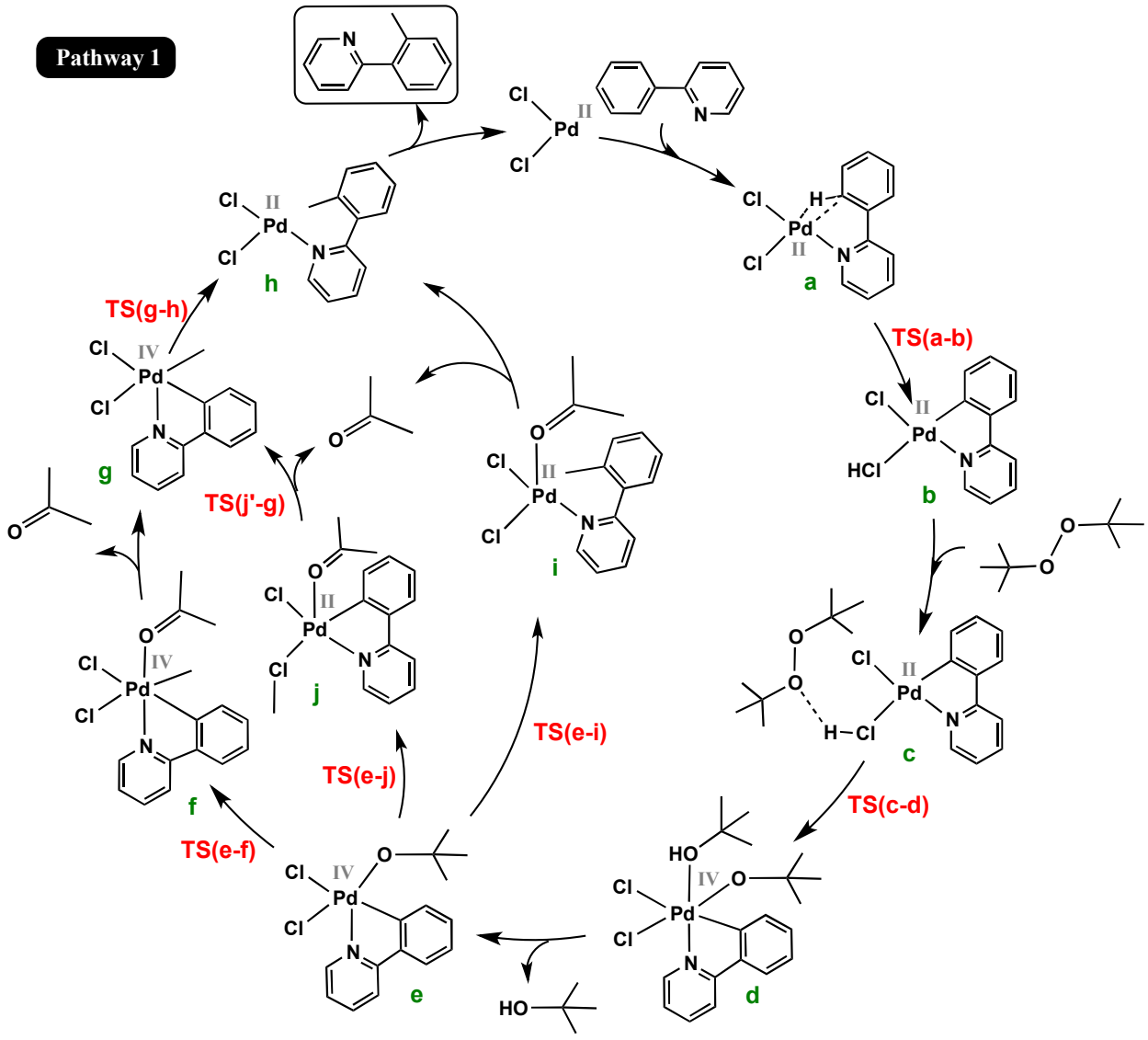

Scheme 2 General mechanism for Pd(II)-catalyzed *ortho*-methylation of 2-phenylpyridine through pathway 1 wherein the coordination of 2-phenylpyridine is prior to peroxide coordination.

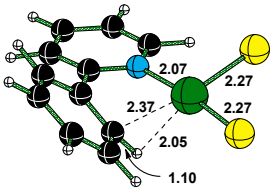

a (0.0)

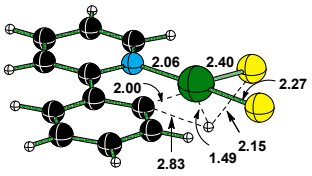

TS(a-b) (34.9)

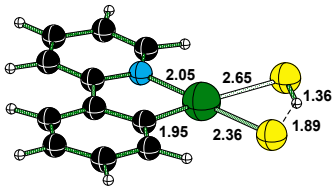

b (0.0)

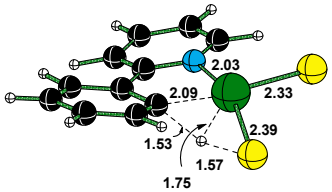

TS(a-b′) (24.9)

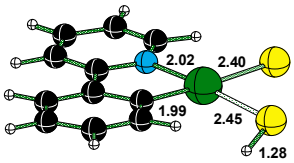

b′ (12.6)

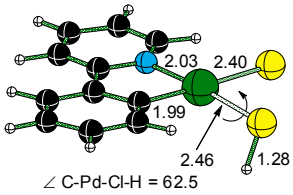

TS(b′-b) (13.0)

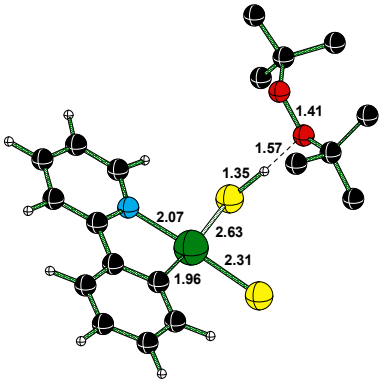

c (3.2)

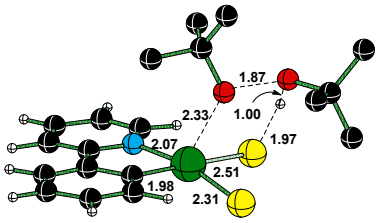

TS(c-d) (23.0)

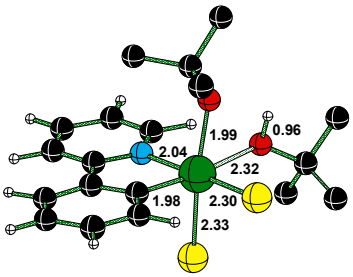

d (-21.1)

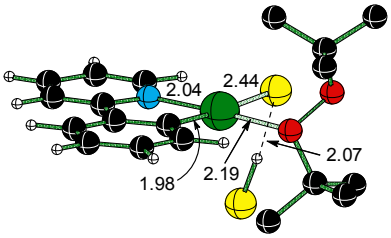

c' (2.0)

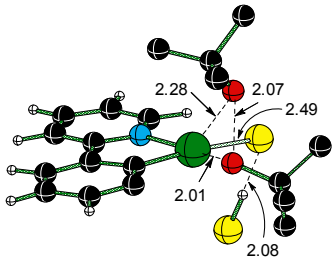

TS(c'-d') (41.4)

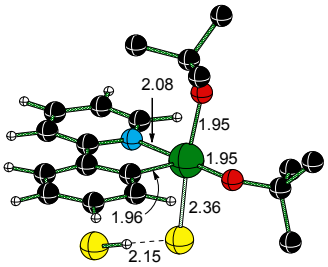

d' (7.3)

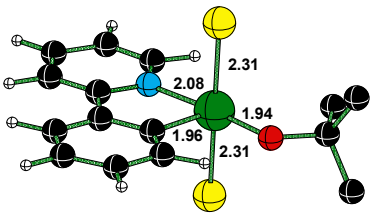

e (-19.4)

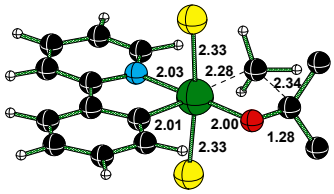

TS(e-f) (13.6)

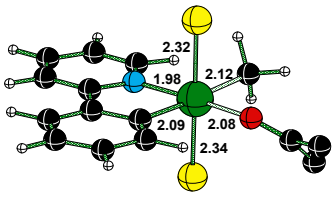

f (-1.1)

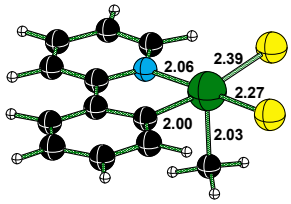

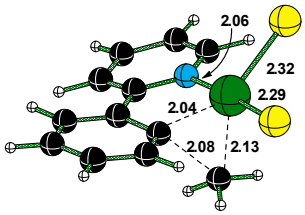

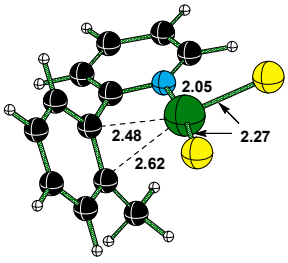

g (-38.1) **TS(g-h)** (-35.1) **h** (-69.8)

Fig. 1 The DFT(mPW1K) optimized geometries of the important transition states and intermediates involved in pathway 1. Relative Gibbs free energies (in kcal/mol) at the M06//mPW1K level of theory with respect to the $PdCl_2$-2-phenylpyridine complex (**a**) are given in parenthesis. [Atom color code: Pd– Green, Cl– Yellow, O– Red, C– Black; distances in Å]

Next, the coordination of *tert*-butyl peroxide to intermediate **b** is examined. The preferred mode of interaction of the peroxide in the initial encounter complex is identified to be through the palladium bound HCl as shown in **c**. This pre-reacting complex consisting of a loosely bound peroxide (**c**) is of higher free energy (by 3.2 kcal/mol) than **b**, though its formation is enthalpically favored (-8.5 kcal/mol).[26] The oxidative insertion of palladium to the peroxidic linkage provides a hexacoordinate Pd(IV) intermediate **d**. Interestingly, the transition state for peroxide activation by palladium is found to involve a simultaneous O–O bond cleavage and protonation of one of the peroxide oxygens by palladium-bound HCl, as shown in **TS(c-d)**. The geometrical features suggest the involvement of a late transition state, as evident from the transfer of the hydrogen from HCl to the peroxide oxygen, which is nearly complete. The transition state **TS(c-d)** leads to an exoergic intermediate **d** with a *tert*-BuOH ligand bound to palladium.[27] The activation barrier for the insertion of palladium to the peroxide bond is found to be 19.8 kcal/mol. Another possibility for this step involves the oxidative addition of Pd into O–O bond first, which will be followed by H-transfer from chloride to the *tert*-butoxy group leading to the formation of intermediate **d**. The pre-reacting complex (**c'**) for the oxidative addition is identified to involve coordination of one of the peroxide oxygen with Pd. However, the transition state for the oxidative addition **TS(c'-d')** is found to be of higher energy than **TS(c-d)**.[28] The O–O bond cleavage assisted by simultaneous proton transfer as in **TS(c-d)** is evidently more feasible. The subsequent release of *tert*-butanol gives intermediate **e** with a *tert*-butoxide bound

to palladium.[29] A β-methyl migration through **TS(e-f)** leads to a vital hexacoordinate Pd(IV)-methyl intermediate **f** with an elementary step activation barrier of 33 kcal/mol.[30] The subsequent release of a molecule of acetone generates a pentacoordinate Pd(IV) species **g** which could be regarded as the active species capable of methylating the aryl ring.[31] The palladium-methyl intermediate **g** is common for different catalytic pathways considered in this study (*vide supra*). The next step is a classic reductive elimination which involves the transfer of the methyl group from palladium to the aryl carbon as shown in **TS(g-h)**. The activation barrier for this process is found to be 3 kcal/mol. In the resulting product complex **h**, $PdCl_2$ is bound to the aryl group through the Pd-N bond besides an η_2 interaction with the aryl moiety. A direct conversion of **f** to **h**, involving reductive elimination is found to be of higher energy.[32]

The summary of the computed energies of all the key stationary points is provided in Table 1. It is evident that the β-methyl migration involving the transfer for the methyl group from the *tert*-butoxide to palladium via **TS(e-f)** has the highest activation barrier (33.0 kcal/mol) and is likely the rate determining step of the reaction. Such high activation barriers is conspicuously in line with the experimentally noted requirements of higher reaction temperatures.[13b]

Table 1 Relative Energies of the Transition States and Intermediates Involved in the Methylation of 2-Phenyl Pyridine Computed at the M06 Level of Theory for Pathway 1[a]

TS / Intermediates	M06//mPW1K	
	ΔH	ΔG
a	0.0	0.0
TS(a-b)	33.6	34.9
b	-0.1	0.0
TS(a-b′)	23.8	24.9
b′	12.9	12.6

TS(b-b′)	12.5	13.0
c	-8.5	3.2
TS(c-d)	7.6	23.0
d	-36.1	-21.1
c'	-10.0	2.0
TS(c'-d')	28.8	41.4
d'	-4.9	7.3
e	-19.4	-19.4
TS(e-f)	10.9	13.6
f	-1.4	-1.1
g	-25.4	-38.1
TS(g-h)	-23.4	-35.1
h	-55.5	-69.8
Product	-55.2	-68.6
TS(e-i)	45.7	47.7
i	-73.7	-75.3
TS(e-j)	18.4	19.5
j	-55.9	-60.9
j′	-46.5	-61.4
TS(j′-g)	-11.8	-24.5

[a] Energies (in kcal/mol) are with respect to $PdCl_2$-substrate complex (**a**).

In addition to the above-mentioned methyl transfer process, we have examined a reductive elimination possibility wherein one of the methyl groups of the *tert*-butoxy ligand gets directly transferred to the aryl ring as shown in **TS(e-i)** in Fig. 2.[33] The proximity of the methyl groups of the *tert*-butyl as well as the corresponding C–C bond distances indicates that the methyl transfer takes place without a direct C–C bond activation in the alkoxy group.[34] As expected, the associated activation barrier for this pathway is as high as 67 kcal/mol. The expulsion of a molecule of acetone from intermediate **i** will furnish a product complex **h** similar to that described earlier.

Another curious variation in pathway 1 emanating from the palladium butoxide intermediate **e** is examined wherein a methyl group transfer to the chloride occurs first, as shown in **TS(e-j)** (Fig. 2). The activation barrier for this process is found to be as high as 39 kcal/mol.

This process is also found to accompany the expulsion of acetone as evident from the weak coordination of acetone in intermediate **j** eventually leading to the formation of **j′**. Subsequently, a methyl transfer in **j′** to palladium gives rise to palladium methyl active species **g**. The barrier for methyl transfer involving **TS(j′-g)** is 37 kcal/mol. Evidently, this route for methylation of the aryl ring can be ruled out due to the high barrier associated with the generation of the active precursor **j**.[35]

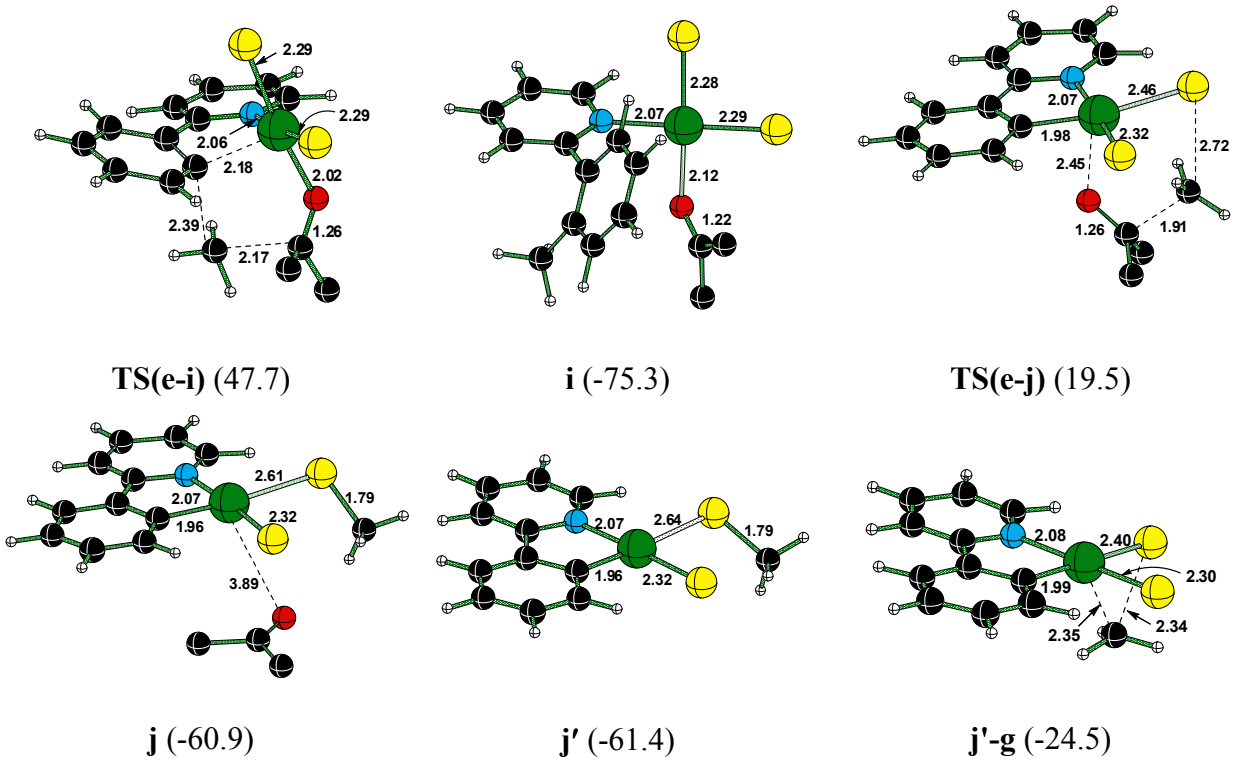

TS(e-i) (47.7) **i** (-75.3) **TS(e-j)** (19.5)

j (-60.9) **j′** (-61.4) **j'-g** (-24.5)

Fig. 2 The DFT(mPW1K) optimized geometries of the transition states and intermediates involving direct methyl transfer or through the chloride ligand. Relative Gibbs free energies (in kcal/mol) at the M06//mPW1K level of theory with respect to the $PdCl_2$-substrate complex are given in parenthesis.

Participation of *tert*-Butoxy Radical Generated from the Peroxide

An equally important possibility within pathway 1 can be envisaged as beginning with the palladacycle intermediate **e**. The intermediate **e** with palladium-bound *tert*-butoxide can undergo reductive elimination to form an aryl ether as the final product (Fig. 3). Interestingly, the relative energy of this TS for the C–O bond formation (**TS(e-e$_{oc}$)**) is -6.2 kcal/mol (13.2 kcal/mol of activation energy), which is lower than the C–C bond activation and β-methyl migration of the methyl group from the *tert*-butoxide to palladium (**TS(e-f)**) presented in the previous section. The resulting aryl ether (**e$_{oc}$**) is as low energy (-62.1 kcal/mol) as the methylated 2-phenyl pyridine noted in the concerted pathway. Hence, the concerted pathway 1 described above is less likely to operate as it should have provided aryl ether than what was observed experimentally.

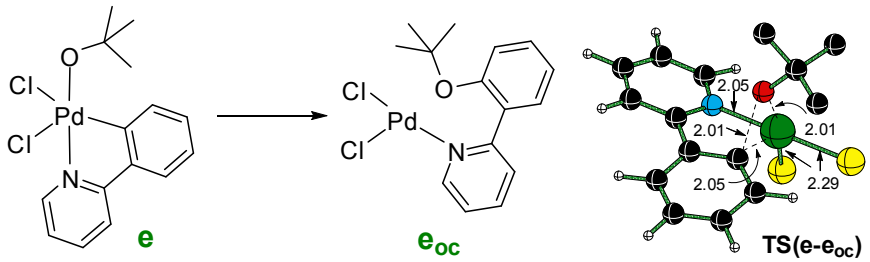

Fig. 3 Possibility of formation of an aryl ether in Pathway 1 by reductive elimination

Since the present reaction employs peroxides at elevated temperature, the involvement of peroxide radicals should be regarded as a likely possibility. Recent literature reports support the participation of radicals in Pd catalyzed aromatic C-H functionalization reactions.[36] Additional examples closely related to the reaction being examined here, suggested a peroxide-induced radical route for arylation and benzoxylation of 2-aryl pyridines.[37] In view of these and the lack of formation of aryl ether as a product (as predicted by the non-radical pathway), we have examined a radical pathway for $PdCl_2$-catalyzed direct methylation of arenes by using dialkyl peroxides. The radical pathway involving thermal decomposition of peroxide could perhaps

compete with the $PdCl_2$-mediated cleavage of the O–O linkage. It is of importance to reckon that the unimolecular thermal decomposition of *tert*-butyl peroxide is reported to have an activation barrier of ~37-39 kcal/mol.[38] The *tert*-butoxy radicals thus generated can readily combine with $PdCl_2$ or intermediate **b** to yield intermediate **l** or **d'**. The thermal decomposition studies on alkoxy radicals, such as *tert*-butoxy radical, have established that unimolecular dissociation would lead to methyl radical and acetone.[39] Should this be the case, formation of other signature side products like methane, ethane, and isobutylene oxide[40] should have been noticed, in addition to the methylated arene as the product. For example, Kharasch et al. have reported the evolution of methane during the decomposition of *tert*-alkoxy radicals in *tert*-butylbenzene solvent in the range of 130-150 °C.[41] Further, *tert*-butoxy radicals are known to abstract hydrogen atom from a variety of available sources.[42] None of such hydrogen abstraction products were observed in the title reaction as opposed to the formation of methylated arenes, *tert*-butanol, and acetone in quantitative proportions. The activation energy for H-abstraction by methyl radical from alkanes are reported to be in the range of 4–8 kcal/mol[43] while that from arenes are known to be of the order of 15 kcal/mol.[44] It was reported that the reaction fails to operate in the absence of the catalyst. This could be regarded as additional indicator for the direct involvement of $PdCl_2$ in the methylation reaction. Both direct and indirect evidences summarized above render support to both radical and a non-radical pathway. It may be possible that a hybrid pathway, involving radical and non-radical intermediates, is operating.

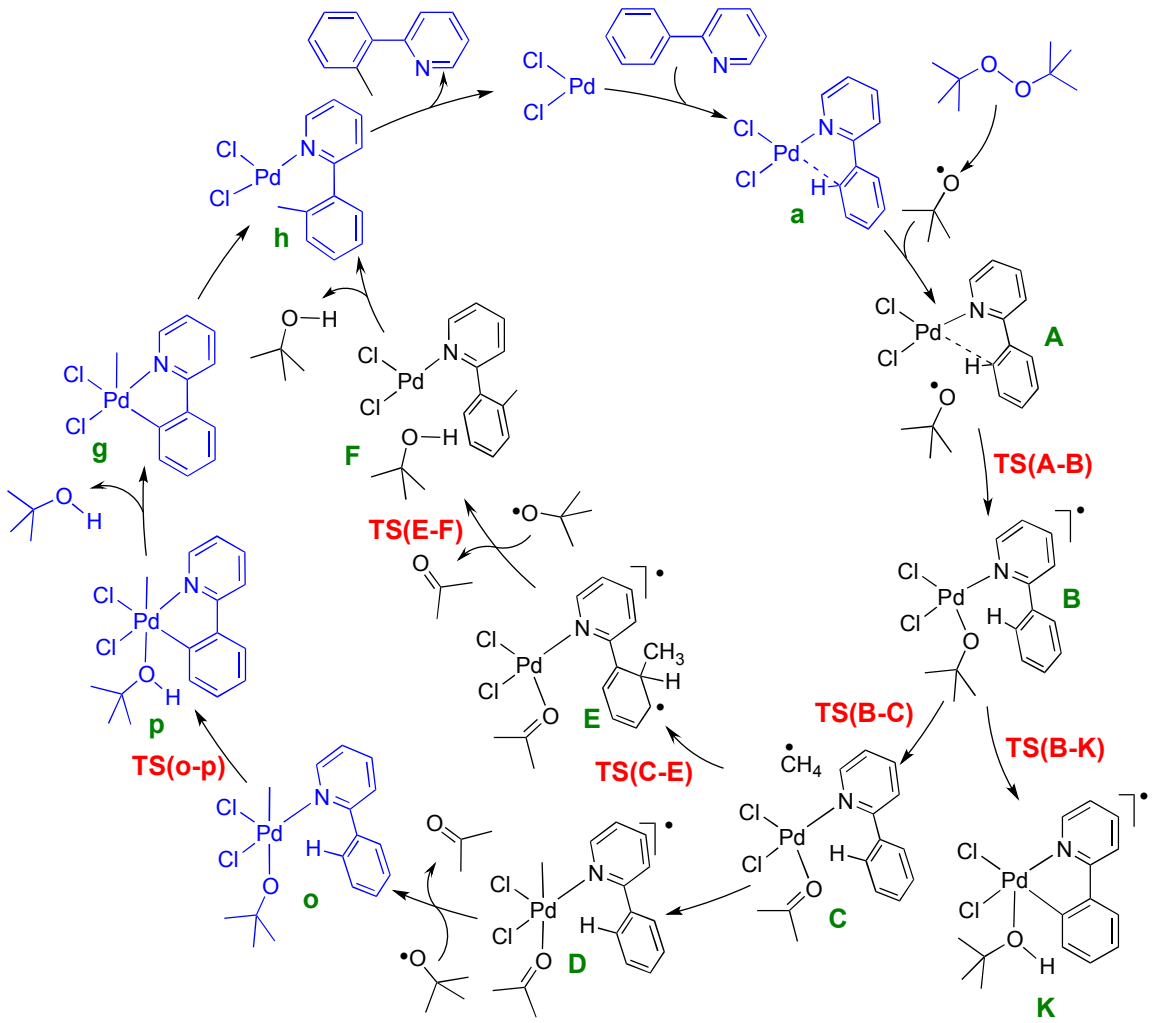

Scheme 3 Mechanism of Pd(II)-catalyzed *ortho*-methylation of 2-phenylpyridine via a radical pathway.

The activation barrier for homolytic cleavage of O–O bond had been found to be 25.5 kcal/mol (Table 2, Fig. 4).[45] The initial coordination of the *tert*-butoxy radical to Pd results in weakening of the agostic interaction between the aryl C–H bond of 2-phenylpyridine and Pd in intermediate **a** (Scheme 3). The pre-reacting complex (**A**) involving the interaction of *tert*-butoxy radical with the catalyst-substrate complex is comparatively higher in energy. The TS for coordination has a low activation barrier and leads to the formation of a lower energy tetra-coordinate Pd intermediate **B**. The Pd-catalyst stabilizes the *tert*-butoxy radical by forming Pd–O

bond as clear lower energy of **B** in comparison to **A**. The intermediate **B** can either undergo C–H bond activation via **TS(B-K)** to a palladacycle intermediate or a C–C bond activation via **TS(B-C)** to furnish a methyl radical. The relative Gibbs free energy of **TS(B-C)** for the formation of methyl radical is 18.6 kcal/mol.[46] The TS for the direct conversion of **B** to a Pd-methyl intermediate **D** through a four-membered geometry is found to be of higher energy.[47] This suggests that the Pd-catalyst helps in the generation of the methyl radical.[48] The barrier for the C–H activation is 13.1 kcal/mol higher than that for the C–C bond activation, suggesting that the generation of a methyl radical is preferred over the formation of palladacycle.[49]

The methyl radical thus generated can either coordinate with Pd or form a bond with 2-phenylpyridine. The binding of the methyl radical to Pd leads to the formation of a lower energy intermediate **D**.[50] Uptake of a *tert*-butoxy radical by **D** can give rise to an interesting overlap between two mechanistic scenarios presented till now. Combination of two radicals can help merge to the non-radical pathway via the formation of a palladium-methyl intermediate **o**, which is found to be energetically favorable (intermediate **o** and the subsequent steps from the same are provided in pathway 2, *vide infra*). The activation barrier for the subsequent steps such as the C–H bond activation (**TS(o-p)**) and reductive elimination (**TS(g-h)**) are found to be lower as well.[51] The coordination of methyl radical to palladium in intermediate **C** appears to be necessary for the ensuing C–H activation, as the alternative possibility such as the addition of the methyl radical to the *ortho*-aryl carbon of 2-phenylpyridine via **TS(C-E)** is of higher energy (Table 2).[52] The next step involves hydrogen abstraction by *tert*-butoxy radical leading to aromatization and the formation of intermediate **F**. Again, the relative Gibbs free energy of **TS(E-F)** is of the order of 21 kcal/mol, suggesting a radical recombination route leading to intermediate **o** is more likely.[53]

An instructive comparison at this juncture is between the Gibbs free energies of **TS(C-E)** and **TS(E-F)** in the radical pathway with that of **TS(o-p)** and **TS(g-h)** in the non-radical route. The relative energy of **TS(o-p)** is only 3.7 whereas that of **TS(E-F)** is 21.0 kcal/mol. Further in the nonradical species **o'** (lowest energy conformer of intermediate **o**) is of lower energy than intermediate **E**. Hence, it is highly suggestive that after the generation of the methyl radical, the reaction proceeds through a non-radical pathway (pathway-A).[54] Equally interesting is to note that the TS for the formation of methane **TS(C-L)** from the intermediate **C** is higher in energy than the other routes available to **C**. This is in line with the fact that no other products, other than methylated 2-phenylpyridine was observed under the experimental conditions.

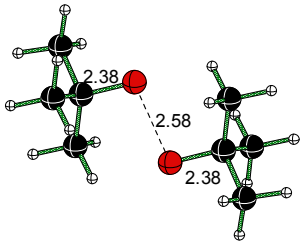

$TS_{Peroxide}$ (25.5)

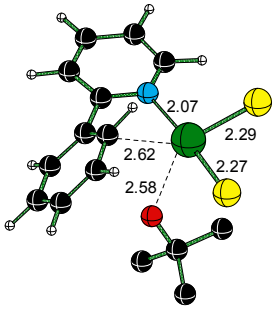

TS(A-B) (22.4)

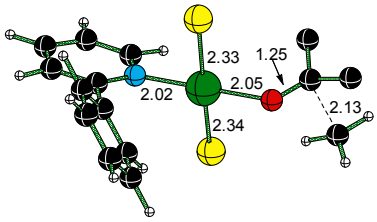

TS(B-C) (18.6)

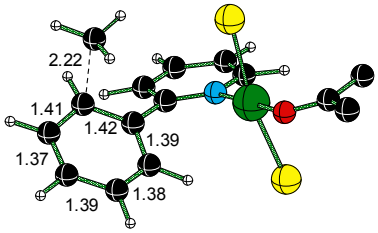

TS(C-E) (20.2)

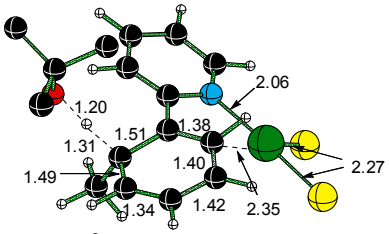

^{3}TS(E-F) (21.0)

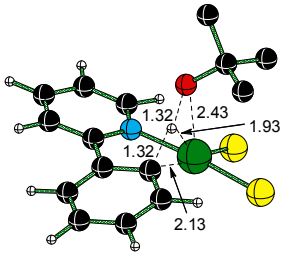

TS(B-K) (31.7)

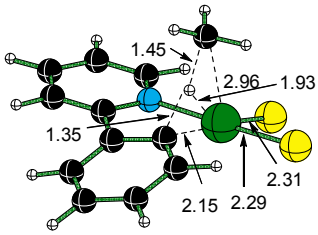

TS(C-L) (26.8)

Fig. 4 The DFT(mPW1K) optimized geometries of transition states involved in the radical pathway. The relative Gibbs free energies (in kcal/mol) at the M06//mPW1K level of theory with respect to $PdCl_2$-2-phenylpyridine and *tert*-butyl peroxide are given in parenthesis.

Table 2: Relative Energies of the Transition States and Intermediates Involved in the Methylation of 2-Phenylpyridine Computed at the M06 Level of Theory for Radical Pathway[a]

TS / Intermediates	M06//mPW1K	
	ΔH	ΔG
$\mathbf{TS_{Peroxide}}$ [b]	28.1	25.5
$\mathbf{Int_{Peroxide}}$ [b]	30.0	24.4
A	24.1	19.6
TS(A-B)	24.6	22.4
B	8.6	6.0
TS(B-C)	20.9	18.6
C	15.8	7.0
D	5.2	-0.5
TS(C-E)	23.9	20.2
E	0.4	-2.9
^{3}**E'** [c]	17.8	10.2
^{3}**TS(E-F)** [c]	23.5	21.0
^{3}**F** [c]	-39.2	-48.1
^{1}**F**	-54.6	-60.6
TS(B-K)	30.9	31.7
K	5.6	4.9
TS(C-L)	42.0	26.8
L	15.8	-5.1

[a] Energies (in kcal/mol) are with respect to $PdCl_2$-2-phenylpyridine and *tert*-butyl peroxide. [b] The energies are with respect to *tert*-butyl peroxide. [c] TS is obtained only in the triplet state. **E'** intermediate is formed by addition of *tert*-butoxy radical to **E**.

Pathway 2: Catalyst Coordination to *tert*-butylperoxide

In pathway 2, the coordination of peroxide to $PdCl_2$ is considered as occurring ahead of its binding with 2-phenylpyridine, as shown in Scheme 4. The key events in this catalytic cycle begins with the cleavage of the peroxide bond. This O–O cleavage can takes place either through

(i) the involvement of Pd(II) catalyst, or (ii) via thermal decomposition under the reaction conditions. In the first possibility, the reaction proceeds with the formation of a pre-reacting complex (**k**), which is exoergic with respect to $PdCl_2$ and *tert*-butyl peroxide (Fig. 5).[55] Interestingly, the $PdCl_2$-substrate complex **a** noted earlier in pathway 1 is thermodynamically more stable than intermediate **k**. The natural bond orbital analysis indicates a significant electron delocalization from n_O to $\sigma^*_{Pd–Cl}$ in **k**, which probably contributes toward the large binding enthalpy, as computed.[56] The relative Gibbs free energy of the transition state for the oxidative insertion of Pd(II) leading to the cleavage of the peroxo bond **TS(k-l)** is found to be 41.6 kcal/mol (Table 3). Equally instructive is to note the high enthalpic ($\Delta H^{‡}$ = 24.0 kcal/mol) and free energy ($\Delta G^{‡}$ = 23.5 kcal/mol) of activation for the oxidative insertion with respect to the pre-reacting complex **k**. The initial role of Pd(II) catalyst here can be ascribed as increasing the probability for the peroxo bond cleavage by forming a relatively stabilized pre-reacting complex (**k**). The comparison of the geometric parameters of the transition state with that of the reactant and the product indicates the involvement of a late transition state. The resultant intermediate **l** is identified to exhibit a favorable spatial disposition for methyl transfer. For instance, one of the *tert*-butyl groups in **l** orients in such a way that the Pd···C_γ distance is only 2.83 Å.

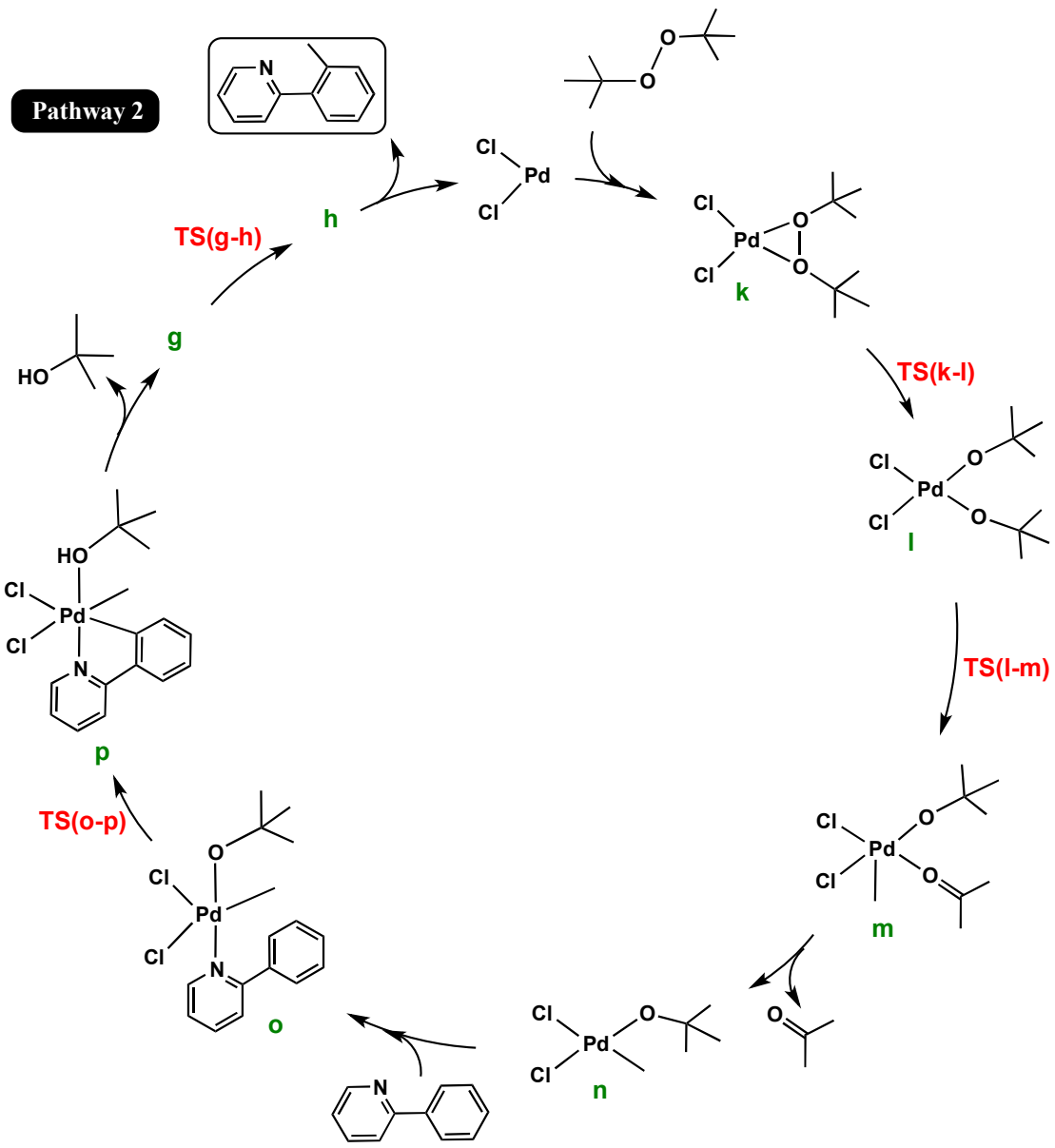

Scheme 4 A mechanistic alternative for Pd(II)-catalyzed *ortho*-methylation of 2-phenylpyridine through pathway 2 wherein the coordination of *tert*-butylperoxide occurs prior to that of 2-phenylpyridine coordination.

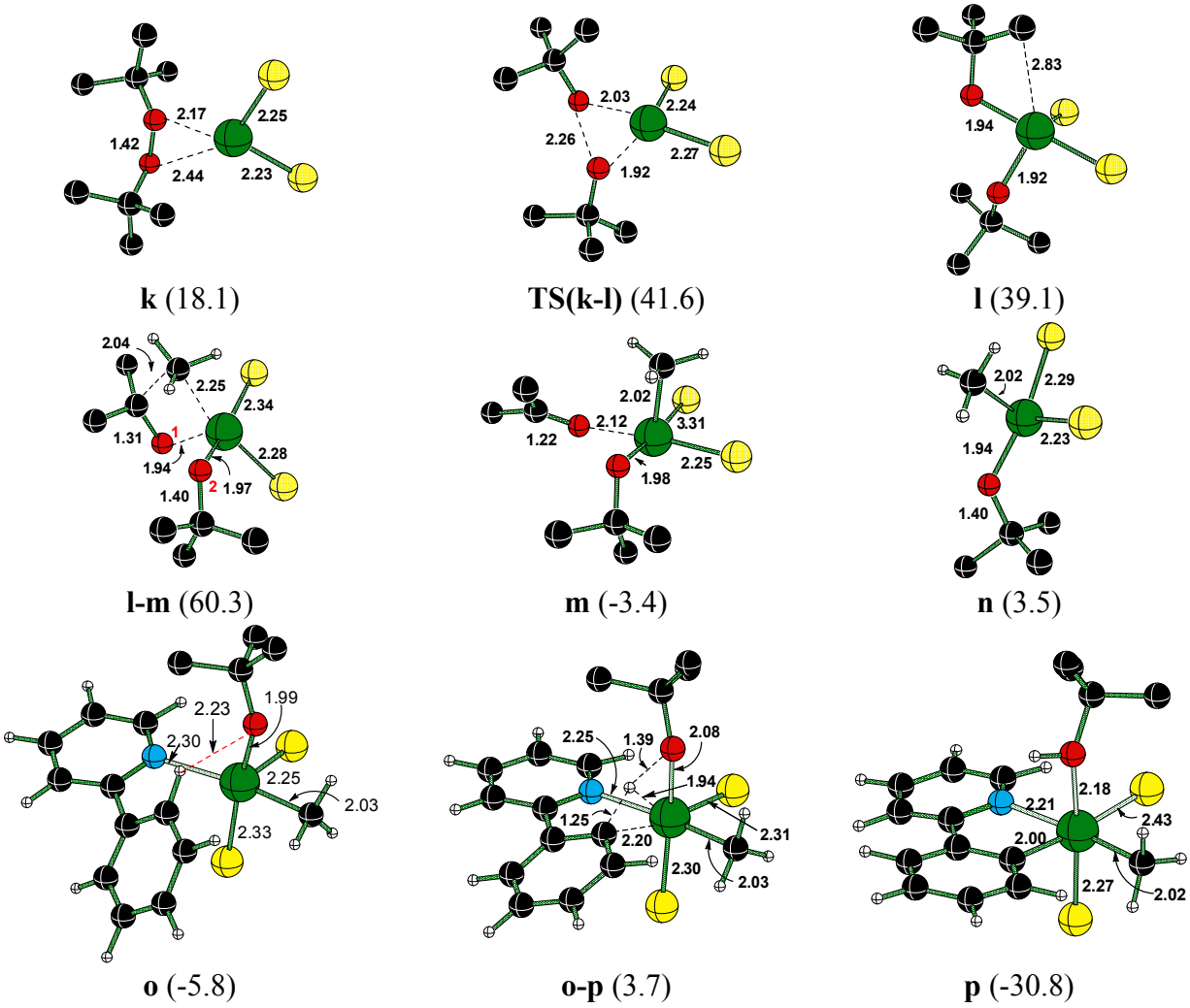

Fig. 5 The DFT(mPW1K) optimized geometries of key transition states and intermediates for the oxidative insertion of Pd(II) to *tert*-butyl peroxide, β-methyl migration and C–H activation in pathway 2. The relative Gibbs free energies (in kcal/mol) at the M06//mPW1K level of theory with respect to $PdCl_2$-2-phenylpyridine and *tert*-butyl peroxide are given in parenthesis.

The subsequent migration of the β-methyl group in the Pd(IV) dibutoxy dichloro intermediate **l** presents a relatively higher energy transition state. The free energy of **TS(l-m)** is about 60 kcal/mol which leads to a palladium methyl intermediate (**m**). The geometrical parameters of this crucial transition state, as provided in Fig. 5, convey certain interesting

features. While the distances along the desired reaction coordinate is quite characteristic of a methyl transfer from the *tert*-butyl carbon to palladium, an elongated Pd–O1 bond length indicates that a concomitant expulsion of a molecule of acetone is quite likely in this step. The palladium-methyl intermediate **m**, with a bound acetone molecule, is found to be significantly lower in energy than its preceding dialkoxy intermediate (**l**). The complete removal of acetone results a higher energy intermediate **n**.[57] In this reaction sequence (pathway 2), the uptake of 2-phenylpyridine leading to a pre-reacting complex **o'** is considered at this stage. The intermediate **o'** is another rotamer of **o** shown in Fig. 5. The coordination of 2-phenylpyridine to **n** is found to be favorable.[58] In order to enable the proton transfer from the aryl ring to the departing *tert*-butoxide in the next step, a rotation around the biaryl C–C bond appears desirable. A low energy torsional transition state **TS(o'-o)** that converts **o′** to another energetically close lying intermediate **o** is located.[59] The complex **o** exhibits a hydrogen-bonding interaction between the aryl hydrogen and the *tert*-butoxy oxygen.

Table 3 Relative Energies[a] of the Transition States and Intermediates Involved in the Methylation of 2-Phenylpyridine Computed at the M06 Level of Theory for Pathway 2

TS / Intermediates	M06//mPW1K	
	ΔH	ΔG
k	18.5	18.1
TS(k-l)	42.5	41.6
l	40.0	39.1
TS(l-m)	59.6	60.3
m	-1.7	-3.4
n	18.9	3.5
o'	-8.4	-9.9
o	-5.2	-5.8
TS(o-p)	2.8	3.7
p	-30.6	-30.8

[a] Energies (in kcal/mol) are with respect to $PdCl_2$-2-phenylpyridine and *tert*-butyl peroxide.

The subsequent transfer of the aryl proton to *tert*-butoxide oxygen in **o** is found to be highly favorable, as revealed by the corresponding transition state **TS(o-p)** (3.7 kcal/mol).[60] The next two steps, i.e., the removal of *tert*-butanol and the methyl transfer are found to be equally favorable as noted in the earlier section. The relative energies of **TS(k-l)**, **TS(l-m)** and intermediate **l** in this pathway are much higher as compared to the relative energies of the stationary points involved in pathway 1. Since intermediate **l** is highly endoergic, the activation barrier for **TS(l-m)** computed should be computed with respect to a lower energy intermediate **k**.[61] This leads to a high activation barrier of the order of 42 kcal/mol for **TS(l-m)**. Hence, this pathway should be regarded as energetically less feasible than pathway 1. The cleavage of *tert*-butyl proxide is therefore expected to take place only after the formation of palladacycle between the catalyst and 2-phenylpyridine.

Pathway 3: Simultaneous Coordination of both substrates followed by the activation of the peroxo bond first

The mechanistic descriptions presented till now invoked the binding of the substrates to the catalyst as taking place in sequence. In the third mechanistic alternative, the coordination of peroxide and 2-phenylpyridine to $PdCl_2$ is considered as occurring ahead of the catalytic action of palladium (Scheme 5). The intermediate **q** in this pathway consists of Pd(II) bound both to 2-phenylpyridine and *tert*-butylperoxide. The intermediates such as **a** and **k**, described earlier as part of pathways 1 and 2, can provide direct access to **q** by the intake of peroxide or 2-phenylpyridine.[62] Comparison of the geometry of **q**, as given in Fig. 6, with that of **a** (which is devoid of peroxide coordination, Fig. 1) reveals that as the peroxide oxygen gets closer to the palladium center, the agostic interaction with the aryl C–H diminishes.[63]

After the coordination of both substrates to $PdCl_2$, the order of activation can vary. For instance, either an oxidative insertion to the peroxide oxygen or a C–H activation of the aryl ring can occur first. Depending on which one of these substrates are activated, two key possibilities designated as pathways 3 and 4, are envisaged. The oxidative cleavage of the peroxide bond prior to the aryl C–H activation leads to pathway 3. In this pathway, the oxidative insertion of palladium to the peroxo bond leads to another intermediate **r**. The energy of transition state **TS(q-r)** indicates a high activation barrier (43.0 kcal/mol) (Table 4).[64] Interestingly, this activation barrier is higher than the similar oxidative insertion barrier to the peroxo bond as noticed in pathway 2 (**k** to **l** conversion). Hence, the uptake of a molecule 2-phenylpyridine by intermediate **l** to give **r** appears more likely.

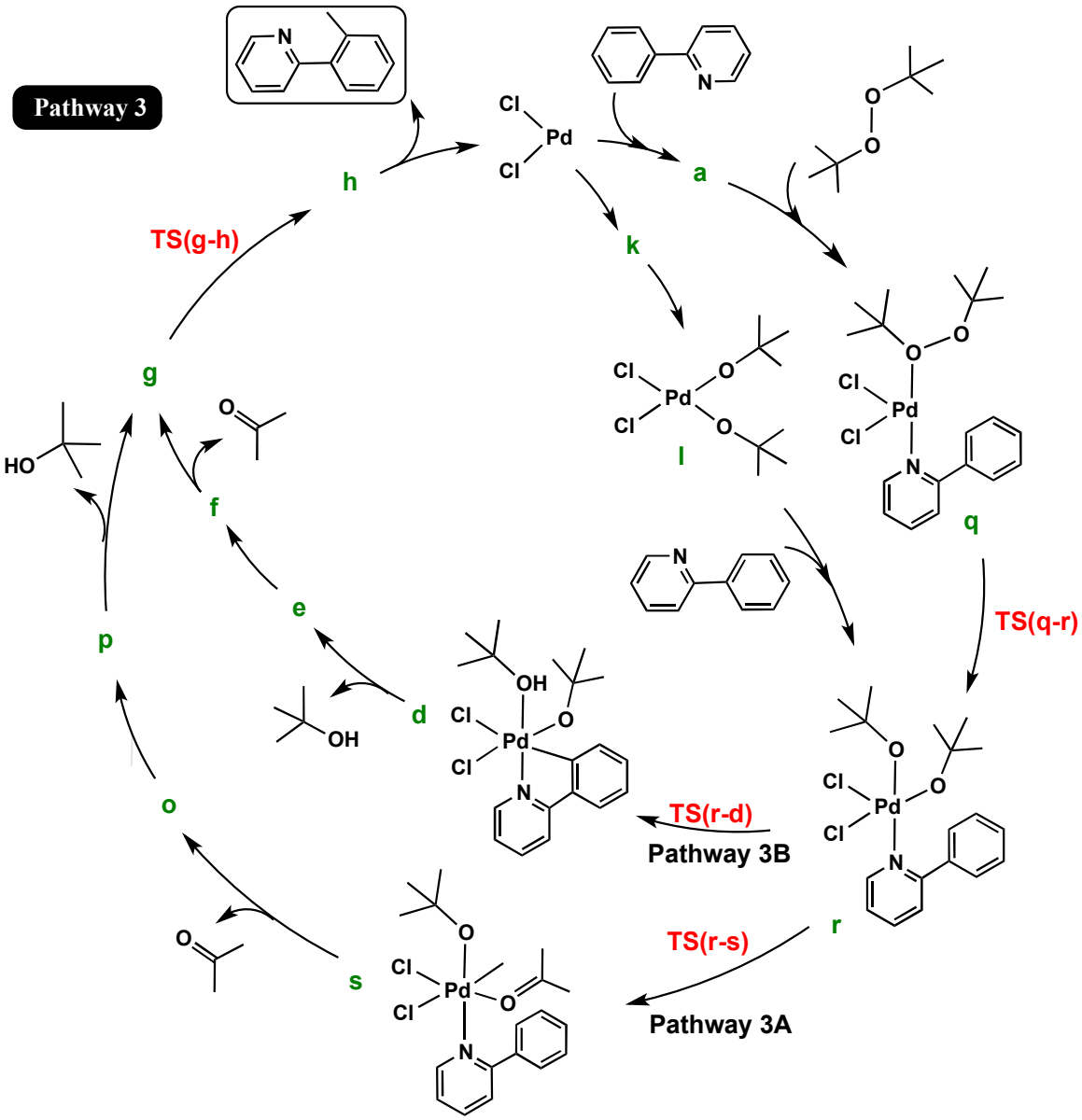

Scheme 5 Another mechanistic alternative for Pd(II)-catalyzed *ortho*-methylation of 2-phenylpyridine through pathway 3 wherein simultaneous coordination of *tert*-butylperoxide and 2-phenylpyridine is considered

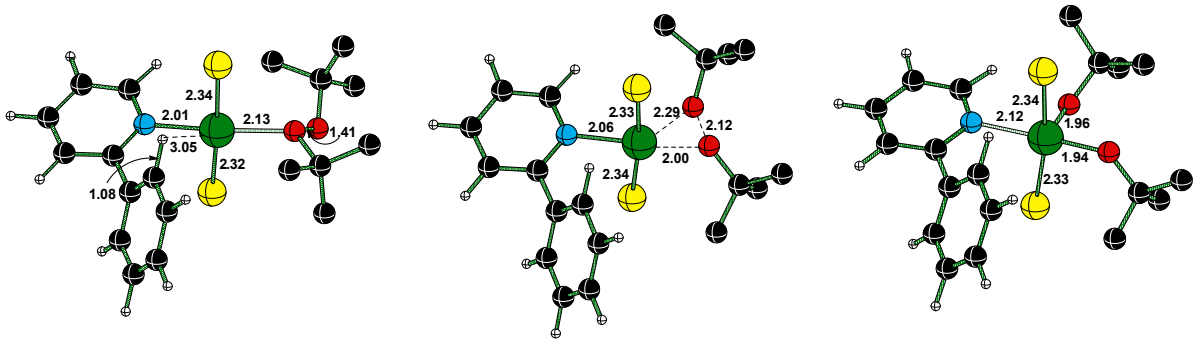

q (-7.2) **TS(q-r)** (35.8) **r'** (20.2)

Fig. 6 The DFT(mPW1K) optimized geometries of the transition state for oxidative insertion to peroxo bond and the corresponding intermediates in pathway 3. Relative Gibbs free energies (in kcal/mol) at the M06//mPW1K level of theory with respect to the $PdCl_2$-2-phenylpyridine complex are given in parenthesis.

The intermediate **r** occupies an important position in this pathway as it can generate either acetone or *tert*-BuOH depending on whether it undergoes a methyl scission (pathway 3A) or hydrogen transfer first (pathway 3B). The computed activation barrier for the β-methyl migration in **r** through **TS(r-s)** is 24.6 kcal/mol. The resultant hexacoordinate Pd(IV) intermediate **s** consists of a weakly bound acetone molecule (Fig. 7). The release of acetone leads to intermediate **o**, which can then continue in the catalytic cycle as described earlier in pathway 2. In an alternative possibility, a proton transfer from 2-phenylpyridine to *tert*-butoxide in intermediate **r** can yield a hexacoordinate intermediate **d**, via **TS(r-d)** as shown in Fig. 7. In the resulting intermediate **d** the nascent *tert*-BuOH is weakly bound to palladium. The activation barrier for this palladium mediated proton transfer is 12.7 kcal/mol. The activation barrier for the direct conversion of **q** to **d**, through a simultaneous O–O bond cleavage and proton transfer from the aryl ring, as shown in **TS(q-d)**, is found to be of considerably higher (61.4 kcal/mol) than in the previously presented pathways for the generation of hexacoordinate intermediate **d**. The geometries of **TS(r-d)** and **TS(q-d)** reveals a key difference in the position of the aryl proton

being transferred, which is nearly perpendicular to the aryl ring in the former while it is in the plane of the ring in the latter case.

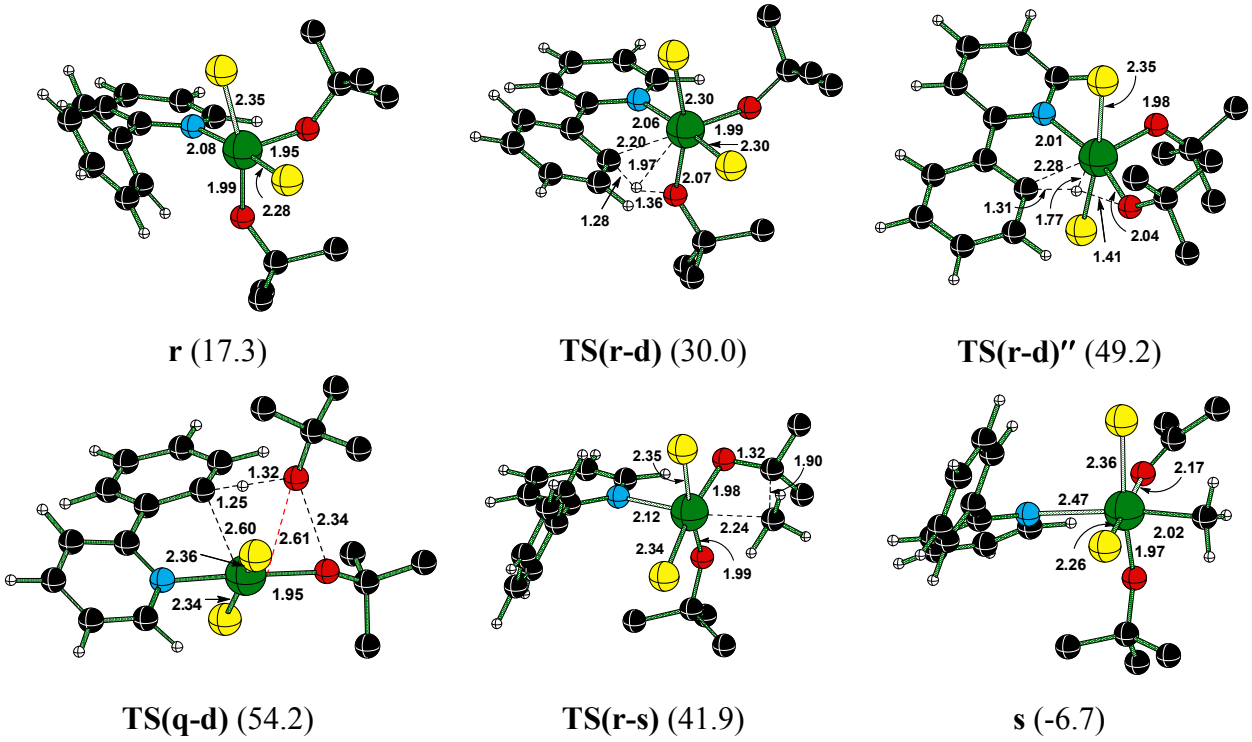

r (17.3) **TS(r-d)** (30.0) **TS(r-d)″** (49.2)

TS(q-d) (54.2) **TS(r-s)** (41.9) **s** (-6.7)

Fig. 7 The DFT(mPW1K) optimized geometries involved in the conversion of **r** to **s** and **d** respectively through methyl and H-transfers and the corresponding transition states in pathways 3A and 3B. Relative Gibbs free energies (in kcal/mol) at the M06//mPW1K level of theory with respect to the $PdCl_2$-2-phenylpyridine complex are given in parenthesis.

Table 4 Relative energies[a] of the Transition States and Intermediates for the Methyl Transfer in 2-Phenylpyridine Involved in Pathway 3

TS / Intermediates	M06//mPW1K	
	ΔH	ΔG
q	-20.6	-7.2
TS(q-r)	21.3	35.8
r	2.5	17.3
TS(r-s)	26.5	41.9

s	-17.7	-6.7
TS(r-d)	13.2	30.0
TS(q-d)	39.3	54.2

[a] Energies (in kcal/mol) are with respect to the $PdCl_2$-2-phenylpyridine complex (**a**).

Akin to the earlier models presented, the transfer of one of the β-methyls from the *tert*-butyl group to palladium through **TS(r-s)** can give rise to intermediate **s**.[65] A comparison of the activation barriers for the conversion of **r** to **s** (24.6 kcal/mol) or to **d** (12.7 kcal/mol) suggests that the formation of *tert*-BuOH **TS(r-d)** is energetically more likely and hence would be preferred over the β-methyl transfer **TS(r-s)**. This indicates that the aryl C–H bond activation is more preferred over the *tert*-butyl C–C bond activation. The subsequent release of *tert*-BuOH from **d** generates intermediate **e** from where the catalytic cycle can proceed as described earlier in the case of pathway 1.

Pathway 4: Simultaneous Coordination of both substrates, followed by the activation of the aryl C–H bond first

In pathway 4, the order of coordination is 2-phenylpyridine followed by *tert*-butylperoxide as shown in Scheme 6. The key stationary point in this pathway is **q** wherein both the reactants are bound to $PdCl_2$. The major difference here is that the oxidative insertion to the aryl C–H occurs ahead of the peroxide cleavage as well as the involvement of a hexacoordinate palladium hydride species **t** (Fig. 8).[66] Intermediate **t** is higher in energy (52.3 kcal/mol) and the relative energy of the corresponding **TS(q-t)** is found to be very high (53.5 kcal/mol) as well (Table 5).[67] The transfer of hydrogen from palladium to one of the peroxide oxygens can result in the removal of *tert*-BuOH. However, the corresponding transition state directly connecting **t** to **d** remained elusive even after repeated attempts. These attempts instead led to a two-step process wherein

the proton is transferred first to the chloride bound to palladium and subsequently to the peroxide oxygen. The **TS(t-u)** leads to an intermediate with a weakly interacting HCl (Fig. 8). The intermediate **u** can convert to **c** which in turn can undergo further reaction as discussed in the case of pathway 1. Another possible mode of C–H activation involving a direct transfer of hydrogen to the adjacent chloride (**TS(q-u)**) is more preferred than through **TS(q-t)** and **TS(t-u)** (Table 5). Two important points relating to this pathway are (i) the activation barrier for **TS(t-u)** conversion is very high, and (ii) intermediate **u** is less stable as compared to similar intermediates identified in the other pathways. Also **TS(q-u)** has high activation barrier (36.3 kcal/mol) than the rate determining step noted earlier in the case of pathway 1. Further, the transition state without the peroxide coordinated to palladium (**TS(q-u)'**) is lower in energy than **TS(q-u)**, which suggests that the C–H activation is preferred in the absence of peroxide coordination to Pd. It is therefore reasonable to conclude that the reaction is less likely to proceed through pathway 4 wherein 2-phenylpyridine coordinates to $PdCl_2$ prior to peroxide coordination.

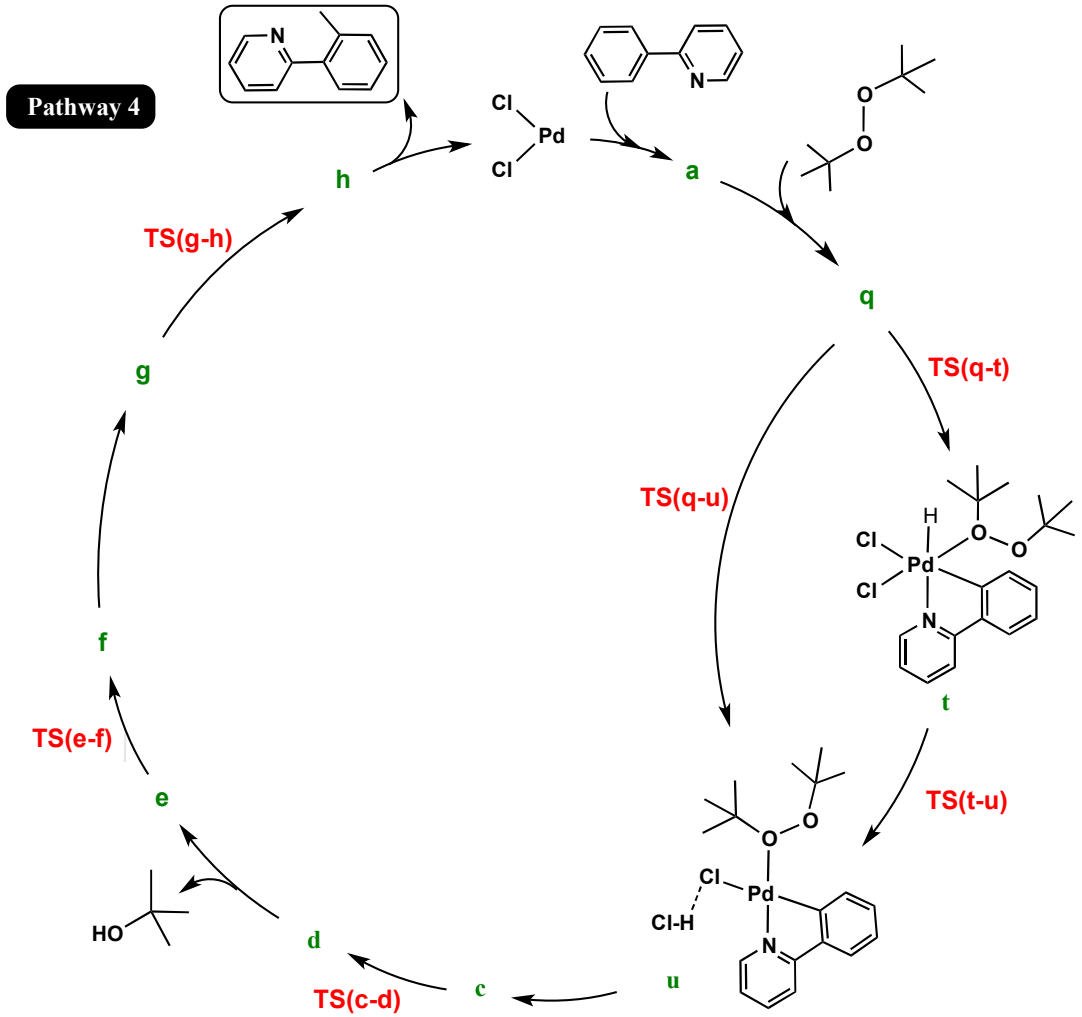

Scheme 6 Another mechanistic alternative for Pd(II)-catalyzed *ortho*-methylation of 2-phenylpyridine through pathway 4 wherein the coordination of 2-phenylpyridine is prior to *tert*-butylperoxide coordination

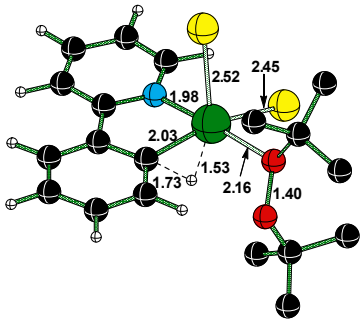

TS(q-t) (53.5)

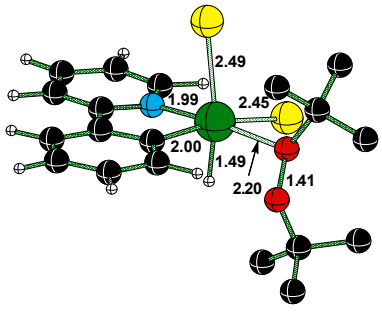

t (52.3)

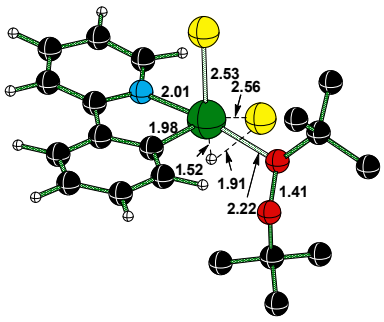

TS(t-u) (52.4)

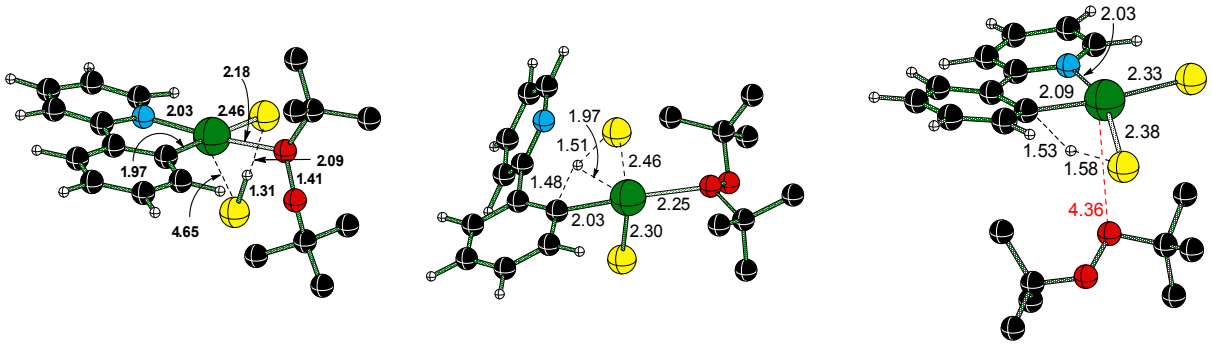

u (0.8) **TS(q-u)** (29.1) **TS(q-u)'** (28.1)

Fig. 8 The DFT(mPW1K) optimized geometries of the important transition states and intermediates for the C–H activation in pathway 4. Relative Gibbs free energies (in kcal/mol) at the M06//mPW1K level of theory with respect to the $PdCl_2$-2-phenylpyridine complex are given in parenthesis.

Table 5 Relative Energies[a] of the Transition States and Intermediates for the Methyl Transfer in 2-Phenylpyridine Involved in Pathway 4

TS / Intermediates	M06//mPW1K	
	ΔH	ΔG
TS(q-t)	37.2	53.5
t	36.2	52.3
TS(t-u)	36.9	52.4
u	-10.9	0.8
TS(q-u)	16.4	29.1
TS(q-u)'	18.5	28.1

[a] Energies (in kcal/mol) are with respect to the $PdCl_2$-2-phenylpyridine complex (**a**).

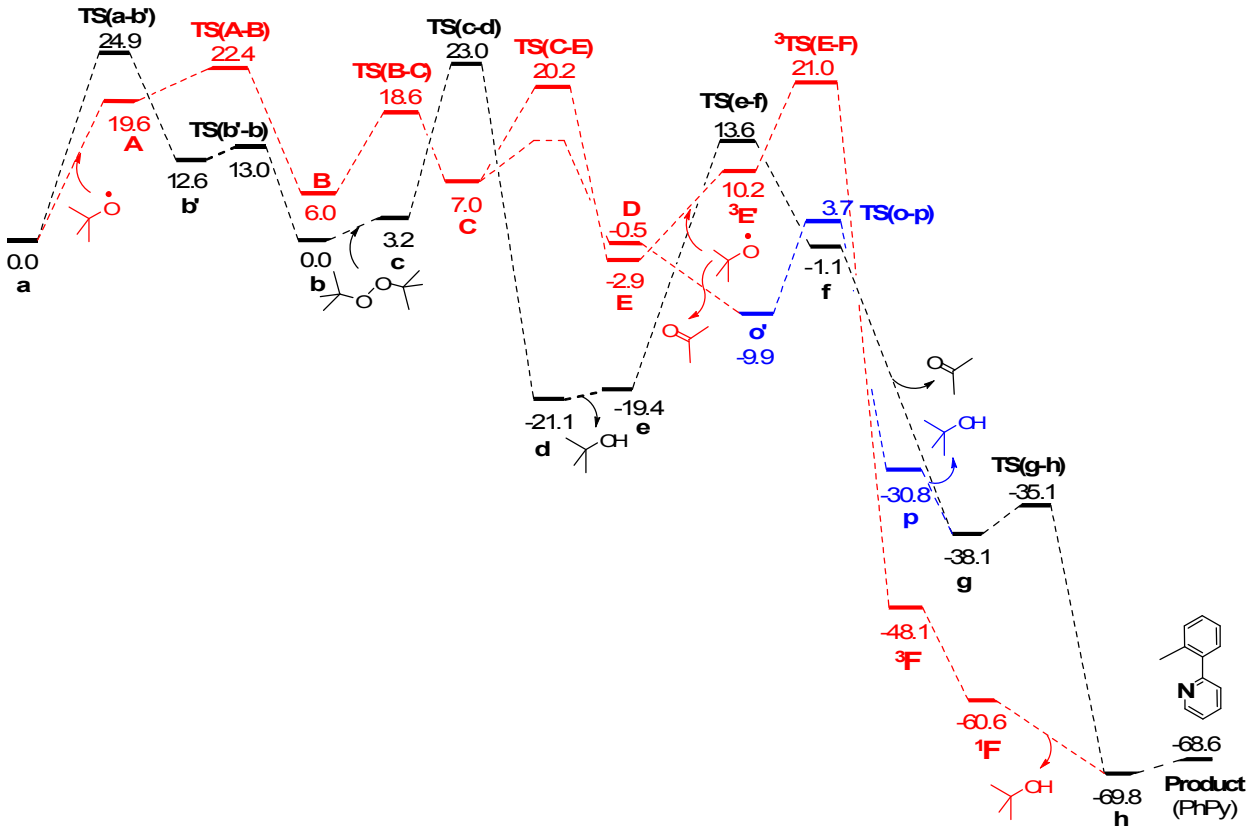

Fig. 9 Combined Gibbs free energy profile diagram for radical (shown in red colour) and non-radical pathway (black and blue) at the M06//mPW1K LANL2DZ(Pd),6-311+G** level of theory. (Note: Energies of homolytic cleavage of peroxide bond are not provided in the energy profile. The TS for methyl radical uptake by palladium in intermediate **C** could not be located).

To enable improved comprehension, the energies of the most preferred pathway is compiled in Fig. 9.[68] The coordination of 2-phenylpyridine to $PdCl_2$ (**a**) is favored over the coordination of peroxide (**k**). On the basis of the relative energies of **TS(a-b)** (as compared to the earlier **TS(k-l)**) it can be concluded that for the coordination of 2-phenylpyridine followed by the C–H bond activation is energetically more preferred over the initial coordination of the peroxide and O–O bond cleavage. The rate determining step in the non-radical pathway of the title reaction is the C–C bond activation of the *tert*-butyl group leading to *β*-alkyl migration via **TS(e-**

f). The reductive elimination step, involving the transfer for methyl group from the metal to the substrate is a low barrier process. Finally, product removal from Pd (catalyst) can be accomplished by the displacement of the same by another molecule of the reactant (2-phenylpyridine).[69]

On the basis of the energetic features summarized in Fig 9, it becomes evident that the reaction will begin by the action of *tert*-butoxy radical on the catalyst-substrate complex (**a**). The transition states and the corresponding intermediate involved in the radical pathway, as depicted using red colour lines, are in general lower in energy than the non-radical pathway. The most interesting feature is that the energetic advantage of the radical pathway continues only up to the formation of a nonradical Pd-methyl intermediate (**o**). The uptake of a methyl radical as well as *tert*-butoxy radical by Pd in two consecutive steps would result in a nonradical Pd-methyl intermediate (**o**). This would be followed by the *ortho* C-H bond activation and cyclometallation leading to palladacycle **g** (*vide infra*). Subsequent reductive elimination that transfers the methyl group from Pd to the aryl group provides the final product complex. The overall energetics provided in Table 2 indicates that the highest activation barrier is for the *tert*-butyl peroxide O–O bond, suggesting that the rate-determining step is prior to the C–H bond activation.

Conclusions

We have elucidated the mechanism of $PdCl_2$-catalyzed direct methylation of 2-phenyl pyridine by *tert*-butyl peroxide by using the M06/6-311+G** level of theory. The energetics of different pathways that differ in terms of the sequence of catalyst ($PdCl_2$) action on the substrate and the involvement of radical intermediates has been compared. In the non-radical pathway (designated as pathway A) the initial coordination of 2-phenylpyridine to $PdCl_2$ has been

identified as more preferred over an alternative possibility of the peroxide coordination ahead of the former. The most preferred non-radical pathway involves (i) *ortho* C–H bond activation of 2-phenylpyridine upon coordination to $PdCl_2$, (ii) coordination of peroxide and oxidative cleavage of the O–O bond and a concomitant transfer of proton from the palladium bound chloro group (HCl) to the *tert*-butoxy group, (iii) the C–C bond activation of *tert*-butyl group leading to the generation of active palladium methyl intermediate, and lastly (iv) the transfer of the methyl group from palladium to the aryl ring furnishes the desired product. As per the computed energetics, the metal-alkyl species (intermediate **g**) could be susceptible to detection under the catalytic conditions. In the other higher energy pathway involving the O–O bond cleavage prior to the coordination with 2-phenylpyridine, the aryl C–H bond activation has been found to be of higher in energy. The coordination of both peroxide and 2-phenylpyridine followed by the catalytic action of palladium has also been found to be energetically less favored. While this mechanism appears reasonable toward rationalizing the quantitative formation ortho methylated 2-phenylpyridine, the lack of formation aryl ethers from a Pd(IV) intermediate prompted us to investigate a potential participation radical intermediates.

Interestingly, a combination of radical and non-radical pathway has been identified as the most likely mechanism. This involves a homolytic cleavage of the peroxide O−O bond, uptake of one of the *tert*-butoxy radicals by palladium and subsequent generation and uptake of the methyl radical by to give a palladium-methyl radical intermediate. The barrier for the *tert*-butyl C−C bond cleavage in the radical intermediate is found to be lower as compared to that in the non-radical pathway. A combination between the palladium-methyl radical intermediate with the second molecule of *tert*-butoxy radical provides a non-radical intermediate. A C-H activation reaction would lead to a palladacycle intermediate while an ensuing reductive elimination

furnishes the final product. The involvement of free radical seems to be necessary for the C–C bond activation, which otherwise exhibits higher activation barrier under non-radical conditions.

References

1 For recent reviews on palladium catalyzed reactions see: (a) F. Pan, Z.-J. Shi, *ACS Catal.*, 2014, **4**, 280; (b) C. E. I. Knappke, A. J. V. Wangelin, *Chem. Soc. Rev.*, 2011, **40**, 4948; (c) H. Li, B.-J. Lia, Z.-J. Shi, *Catal. Sci. Technol.*, 2011, **1**, 191; (d) C. Torborga, M. Beller, *Adv. Synth. Catal.*, 2009, **351**, 3027; (e) M.-N. Birkholz, Z. Frexia, P. W. N. M. van Leeuwen, *Chem. Soc. Rev*., 2009, **38**, 1099; (f) H. Amii, K. Uneyama, *Chem. Rev*., 2009, **109**, 2119; (g) E. M. Beccalli, G. Broggini, M. Martinelli, S. Sottocornola, *Chem. Rev*., 2007, **107**, 5318; (h) C. I. Herrerías, X. Yao, Z. Li, C.-J. Li, *Chem. Rev*., 2007, **107**, 2546.

2 (a) T. D. Senecal, W. Shu, S. L. Buchwald, *Angew. Chem. Int. Ed.*, 2013, **52**, 10035; (b) N. Kambe, T. Iwasakia, J. Teraob, *Chem. Soc. Rev.*, 2011, **40**, 4937; (c) A. C. Frisch, M. Beller, *Angew. Chem. Int. Ed*., 2005, **44**, 674.

3 (a) N. Kuhl, M. N. Hopkinson, J. Wencel-Delord, F. Glorius, *Angew. Chem. Int. Ed.*, 2012, **51**, 10236; (b) C. S. Yeung, V. M. Dong, *Chem. Rev.*, 2011, **111**, 1215; (c) T. W. Lyons, M. S. Sanford, *Chem. Rev.*, 2010, **110**, 1147; (d) X. Chen, K. M. Engle, D.-H. Wang, J.-Q. Yu, *Angew. Chem. Int. Ed.*, 2009, **48**, 5094; (e) Y. J. Park, J.-W. Park, C.-H. Jun, *Acc. Chem. Res*., 2008, **41**, 222; (f) A. M. Díaz-Requejo, P. J. Pérez, *Chem. Rev*., 2008, **108**, 3379.

4 (a) V. Lanke, K. R. Prabhu, *Org. Lett.*, 2013, **15**, 2818; (b) S. I. Kozhushkov, L. Ackermann, *Chem. Sci.*, 2013, **4**, 886; (c) G. Song, F. Wang, X. Li, *Chem. Soc. Rev.*, 2012, **41**, 3651; (d) J. F. Hooper, A. B. Chaplin, C. González-Rodríguez, A. L. Thompson, A. S. Weller, M. C. Willis, *J. Am. Chem.Soc.*, 2012, **134**, 2906; (e) P. B. Arockiam, C. Bruneau, P. H. Dixneuf, *Chem. Rev.*,

2012, **112**, 5879; (f) D. A. Colby, R. G. Bergman, J. A. Ellman, *Chem. Rev.*, 2010, **110**, 624; (g) N. A. Foley, J. P. Lee, Z. Ke, T. B. Gunnoe, T. R. Cundari, *Acc. Chem. Res*., 2009, **42**, 585; (h) M. Beller, J. Seayad, A. Tillack, H. Jiao, *Angew. Chem. Int. Ed*., 2004, **43**, 3368.

5 (a) R. Martin, S. L. Buchwald, *Acc. Chem. Res.*, 2008, **41**, 1461; (b) P. Lloyd-Williams, E. Giralt, *Chem. Soc. Rev*., 2001, **30**, 145; (c) N. Miyura, A. Suzuki, *Chem. Rev*., 1995, **95**, 2457.

6 (a) A. de Meijere, F. E. Meyer, *Angew. Chem. Int. Ed.*, 2004, **33**, 2379; (b) R. F. Heck, J. P. Noley, Jr., *J. Org. Chem*., 1972, **37**, 2320.

7 (a) W.-N. Li, Z.-L. Wang, *RSC Adv.*, 2013, **3**, 25565; (b) M. E. Limmert, A. H. Roy, J. F. Hartwig, *J. Org. Chem*., 2005, **70**, 9364; (c) J. Huang, S. P. Nolan, *J. Am. Chem. Soc*., 1999, **121**, 9889; (d) R. J. P. Corriu, J. P. Masse, *J. Chem. Soc. Chem. Commun*., 1972, 144; (e) K. Tamao, K. Sumitani, M. Kumada, *J. Am. Chem. Soc*., 1972, **94**, 4374.

8 For reviews in this field see (a) N. I. Nikishkin, J. Huskens, W. Verboom, *Org. Biomol. Chem.*, 2013, **11**, 3583; (b) B. Li, P. H. Dixneuf, *Chem. Soc. Rev.*, 2013, **42**, 5744; (c) R. Jana, T. P. Pathak, M. S. Sigman, *Chem. Rev.*, 2011, **111**, 1417; (d) T. Ren, *Chem. Rev*., 2008, **108**, 4185; (e) L. Yin, J. Liebscher, *Chem. Rev*., 2007, **107**, 133; (f) I. P. Beletskaya, A. V. Cheprakov, *Chem. Rev*., 2000, **100**, 3009; (i) V. Grushin, H. Alper, *Chem. Rev*., 1994, **94**, 1047.

9 (a) C. Amatore, G. L. Duc, A. Jutand, *Chem. Eur. J.*, 2013, **19**, 10082; (b) A. J. J. Lennox, G. C. Lloyd-Jones, *Angew. Chem. Int. Ed.*, 2013, **52**, 7362; (c) B. P. Carrow, J. F. Hartwig, *J. Am. Chem. Soc.*, 2011, **133**, 2116; (d) K. M. Engle, D.-H. Wang, J.-Q. Yu, *J. Am. Chem. Soc.*, 2010, **132**, 14137; (e) N. R. Deprez, M. S. Sanford, *J. Am. Chem. Soc.*, 2009, **131**, 11234; (f) M. C. Kohler, T. V. Grimes, X. Wang, T. R. Cundari, R. A. Stockland, Jr., *Organometallics*, 2009, **28**, 1193; (g) K. L. Hull, M. S. Sanford, *J. Am. Chem. Soc*., 2009, **131**, 9651; (h) E. Alvaro, J. F. Hartwig, *J. Am. Chem. Soc*., 2009, **131**, 7858; (i) Y. Fu, Z. Li, S. Liang, Q.-X. Guo, L. Liu,

Organometallics, 2008, **27**, 3736; (j) R. Álvarez, O. N. Faza, A. R. de Lera, D. J. Cárdenas, *Adv. Synth. Catal*., 2007, **349**, 887.

10 (a) L. Xu, M. J. Hilton, X. Zhang, P.-O. Norrby, Y.-D. Wu, M. S. Sigman, O. Wiest, *J. Am. Chem. Soc.*, 2014, DOI: 10.1021/ja4109616; (b) Y.-F. Yang, G.-J. Cheng, P. Liu, D. Leow, T.-Y. Sun, P. Chen, X. Zhang, J.-Q. Yu, Y.-D. Wu, K. N. Houk, *J. Am. Chem. Soc.*, 2014, **136**, 344; (c) M. García-Melchor, A. A. C. Braga, A. Lledós, G. Ujaque, F. Maseras, *Acc. Chem. Res*., 2013, **46**, 2626; (d) A. Parija, R. B. Sunoj, *Org. Lett.*, 2013, **15**, 4066; (e) D. Katayev, Y.-X. Jia, A. K. Sharma, D. Banerjee, C. Besnard, R. B. Sunoj, E. P. Kündig, *Chem. Eur. J.*, 2013, **19**, 11916; (f) R. Rajeev, R. B. Sunoj, *Dalton Trans.*, 2012, **41**, 8430; (g) B. Butschke, H. Schwarz, *Organometallics*, 2011, **30**, 1588; (h) A. Ishikawa, Y. Nakao, H. Sato, S. Sakaki *Dalton Trans.*, 2010, **39**, 3279; (i) S. Zhang, L. Shi, Y. Ding, *J. Am. Chem. Soc.*, 2011, **133**, 20218; (j) Z. Ke, T. R. Cundari, *Organometallics*, 2010, **29**, 821; (k) D. H. Ess, T. B. Gunnoe, T. R. Cundari, W. A. Goddard, III, R. A. Periana, *Organometallics*, 2010, **29**, 6801; (l) L. Xue, Z. Lin, *Chem. Soc. Rev.*, 2010, **39**, 1692; (m) D. Balcells, E. Clot, O. Eisenstein, *Chem. Rev.*, 2010, **110**, 749; (n) Y. Boutadla, D. L. Davies, S. A. Macgregor, A. I. Poblador-Bahamonde, *Dalton Trans.*, 2009, 5820.

11 (a) P. S. Thuy-Boun, G. Villa, D. Dang, P. Richardson, S. Su, J.-Q. Yu, *J. Am. Chem. Soc.*, 2013, **135**, 17508; (b) S. Y. Zhang, G. He, W. A. Nack, Y. Zhao, Q. Li, G. Chen, *J. Am. Chem. Soc.* 2013, **135**, 2124; (c) S. R. Neufeldt, C. K. Seigerman, M. S. Sanford, *Org.Lett.*, 2013, **15**, 2302.; (d) D. W. Robbins, J. F. Hartwig, *Angew. Chem. Int. Ed.*, 2013, **52**, 933; (e) T. Yao, K. Hirano, T. Satoh, M. Miura, *Angew. Chem. Int. Ed.*, 2012, **51**, 775; (f) L. Ackermann, *Chem. Commun.*, 2010, **46**, 4866; (f) C. Jia, T. Kitamura, Y. Fujiwara, *Acc. Chem. Res*., 2001, **34**, 633.

12 (a) C. J. Engelin, P. Fristrup, *Molecules*, 2011, **16**, 951; (b) S. Lin, C.-X. Song, G.-X. Cai, W.-H. Wang, Z.-J. Shi, *J. Am. Chem. Soc*., 2008, **130**, 12901; (c) V. Ritleng, C. Sirlin, M. Pfeffer, *Chem. Rev*., 2002, **102**, 1731.

13 (a) Y.-H. Zhang, B.-F. Shi, J.-Q. Yu, *Angew. Chem. Int. Ed*., 2009, **48**, 6097; (b) J.-H. Chu, S.-L. Tsai, M.-J. Wu, *Synthesis*, 2009 3757; (c) B. Mariampillai, J. Alliot, M. Li, M. Lautens, *J. Am. Chem. Soc*., 2007, **129**, 15372; (d) A. Martins, D. Alberico, M. Lautens, *Org. Lett*., 2006, **8**, 4827.

14 (a) C.-J. Li, *Acc. Chem. Res*., 2009, **42**, 335; (b) Y. Zhang, J. Feng, C.-J. Li, *J. Am. Chem. Soc*., 2008, **130**, 2900.

15 Such β-carbyl elimination reactions are important tools in activating an otherwise inert C–C bond toward further functionalization. For related examples see (a) J. R. Bour, J. C. Green, V. J. Winton, J. B. Johnson, *J. Org. Chem.*, 2013, **78**, 1665; (c) Y. Zhu, H. Yan, L. Lu, D. Liu, G. Rong, J. Mao, *J. Org. Chem.*, 2013, **78**, 9898; (b) K. Ruhland, *Eur. J. Org. Chem.* 2012, 2683; (d) W. Jin, Z. Yu, W. He, W. Ye, W.-J. Xiao, *Org. Lett*., 2009, **11**, 1317; (e) L. Xue, K. C. Ng, Z. Lin, *Dalton Trans*., 2009, 5841; (f) P. Zhao, J. F. Hartwig, *Organometallics*, 2008, **27**, 4749; (e) J. F. Hartwig, *Inorg. Chem*., 2007, **46**, 1936.

16 (a) A. Maleckis, J. W. Kampf, M. S. Sanford, *J. Am. Chem. Soc.* 2013, **135**, 6618; (b) A. J. Hickman, M. S. Sanford, *Nature*, 2012, **484**, 177; (c) N. A. B. Juwaini, J. K. P. Ng, J. Seayad, *ACS Catal.*, 2012, **2**, 1787; (d) X. Wang, D. Leow, J.-Q. Yu, *J. Am. Chem. Soc.* 2011, **133**, 13864; (e) K. Muñiz, *Angew. Chem. Int. Ed.* 2009, **48**, 9412. In the activation of molecular oxygen by palladium complexes, the formation of higher valent palladium intermediates is reported. See for example C. Adamo, C. Amatore, I. Ciofini, A. Jutand, H. Lakmini, *J. Am. Chem. Soc*., 2006, **128**, 6829.

17 (a) M. J. Frisch, *et al.* Gaussian 03, Revision C.02, Gaussian, Inc., Wallingford CT, 2004. (b) M. J. Frisch, *et al.* Gaussian 09 Revision A.02; Gaussian, Inc., Wallingford, CT, 2009. See ESI for the full citation.

18 B. J. Lynch, P. L. Fast, M. Harris, D. G. Truhlar, *J. Phys. Chem. A*, 2000, **104**, 4811.

19 P. J. Hay, W. R. Wadt, *J. Chem. Phys*., 1985, **82**, 299.

20 M. Bertoli, A. Choualeb, D. G. Gusev, A. J. Lough, Q. Major, B. Moore, *Dalton Trans.*, 2011, **40**, 8941; (a) M. A. Fox, R. L. Roberts, T. E. Baines, B. Le Guennic, J. -F. Halet, F. Hartl, D. S. Yufit, D. Albesa-Jove, J. A. K. Howard, P. J. Low, *J. Am. Chem. Soc.*, 2008, **130**, 3566; (b) J. Zhu, G. Jia, Z. Lin, *Organometallics*, 2007, **26**, 1986; (c) E. Ben-Ari, R. Cohen, M. Gandelman, L. J. W. Shimon, J. M. L. Martin, D. Milstein, *Organometallics*, 2006, **25**, 3190; (d) M. A. Iron, A. C. B. Lucassen, H. Cohen, M. E. van der Broom, J. M. L. Martin, *J. Am. Chem. Soc*., 2004, **126**, 11699.

21 Y. Zhao, D. G. Truhlar, *Theor. Chem. Acc.*, 2008, **120**, 215.

22 C. Gonzalez, H. B. Schlegel, *J. Phys. Chem*., 1990, **94**, 5523.

23 (a) A. E. Reed, L. A. Curtiss, F. Weinhold, *Chem. Rev*., 1988, **88**, 899; (b) E. D. Glendening, A. E. Reed, J. E. Carpenter, F. Weinhold, NBO Version 3.1.(Theoretical Chemistry Institute, University of Wisconsin, Madison, WI, 2001.)

24 (a) The C–$H_{agostic}$ distance (1.10 Å) is found to be slightly longer than a typial C–H bond (1.08 Å) away from the palladium center. (b) The NBO analysis at the mPW1K/LANL2DZ, 6-311+G** level of theory confirms the presence of delocalization of $\sigma_{(C–H)}$ to Pd with a second-order perturbative stabilization of 25.4 kcal/mol.

25 All attempts to locate a palladium hydride intermediate through an oxidative C–H insertion collapsed to **b** in which the hydrogen combines with the chloride bound to palladium, resulting in the formation of HCl.

26 The geometry of **c** is obtained through the IRC calculation followed by geometry optimization using the OPT=RCFC option available in Gaussian 09 program.

27 The imaginary frequency pertaining to the reaction coordinate is identified to involve the peroxide O–O bond cleavage and a simultaneous transfer of hydrogen from the Cl to one of the peroxide oxygen while the other peroxide begins to develop a Pd–O bond. Different transition state geometries, which differ in the position of the coordinating HCl and the conformation of the *tert*-butyl group, have been optimized for this step so as to locate the lower energy TS. For additional details see Fig. S7 in ESI.

28 The intermediate **d'** formed through the oxidative addition leads to **d** via a proton transfer from Cl to O of *tert*-butoxy ligand. For more details on proton transfer **TS(d'''-d'''')** and isomeric TS for **TS(c'-d')** see Fig. S8 in ESI.

29 The relative positions of the chloride ligands in intermediate **d** is *syn* while that in **e** it is *anti*. The isomer of **e** with ligand positions same as that in **d** is higher of energy.

30 Other isomeric transition states with different coordination pattern have also been optimized. These are found to be of higher energies. See Fig. S7 in ESI.

31 Note that ligand positions in **g**, after the release of acetone, is different form that in **f**. Only the lowest energy isomer with favorable ligand positions for the next step is provided here. An alternative isomer of **g** with the ligand position same as that in **f** is found to be of slightly higher in energy (0.2 kcal/mol). See Fig. S9 in ESI.

32 The TS with acetone coordinated to Pd (as in intermediate **f**) is higher in energy than the TS in which acetone is not coordinating with Pd. For additional details see Fig. S9 in ESI.

33 In the most preferred isomer of intermediate **e**, the two chloride ligands are *trans* to each other (Fig. 1), whereas **TS(e-i)** demands a *cis* disposition (Fig. 2). Assuming that the ligand reorganization is of lower energy as compared to the other steps in the reaction, we have considered this additional possibility to verify that the lowest energy intermediates and TSs are identified.

34 The C–C bond distances in free *tert*-butyl peroxide and that in intermediate **e** are respectively 1.518 and 1.523 Å at the mPW1K/LANL2DZ, 6-311+G** level of theory.

35 (a) A possibility in which two molecules of 2-phenylpyridine are coordinated to $PdCl_2$ is additionally examined. Although the initial uptake leading to formation of $[PdCl_2(PhPy)_2]$ is favored (-17.5 kcal/mol), the activation barrier for the subsequent steps such as that for the cleavage of the peroxide bond is found to be very high (59.6 kcal/mol). See Fig. S10 in ESI for additional details. Furthermore, the coordination of two 2-phenylpyridine ahead of peroxide is less likely as only one equivalent of this substrate is employed in the reaction while two equivalents of peroxide is introduced into the reaction mixture. (b) The formation of $[Pd(PhPy)_2]$+2HCl by a C–H activation of two 2-phenylpyridine is found to be less feasible as this complex is higher in energy. The corresponding transition state for its formation is also of high energy, see Fig. S11 in ESI for more details.

36 (a) D. Kalyani, K. B. McMurtrey, S. R. Neufeldt, M. S. Sanford, *J. Am. Chem. Soc.*, 2011, **133**, 18566; (b) C.-W. Chan, Z. Zhou, A. S. C. Chan, W.-Y. Yu, *Org. Lett.*, 2010, **12**, 3926. (c) G. Manolikakes, P. Knochel, *Angew. Chem. Int. Ed.* 2009, **48**, 205.

37 (a) W.-Y. Yu, W. N. Sit, Z. Zhou, A. S.-C. Chan, *Org. Lett.*, 2009, **11**, 3174. (b) W.-N. Sit, C.-W. Chan, W.-Y. Yu *Molecules*, 2013, **18**, 4403. (c) A copper-catalyzed N-methylation of amides using *tert*-butyl peroxide also suggested to proceed via a radical pathway. See Q. Xia, X. Liu, Y. Zhang, C. Chen, W. Chen, *Org. Lett.*, 2013, **15**, 3326.

38 J. H. Raley, F. F. Rust, W. E. Vaughan, *J. Am. Chem. Soc*., 1948, **70**, 1336.

39 D. Griller, K. U. Ingold, *Acc. Chem. Res*., 1980, **13**, 317.

40 E. E. Bell, F. F. Rust, W. E. Vaughan, *J. Am. Chem. Soc*., 1950, **72**, 337.

41 M. S. Kharasch, A. Fono, W. Nudenberg, *J. Org. Chem*. 1951, **16**, 105.

42 C. Walling, J. A. McGuinness, *J. Am .Chem. Soc*. 1969, **91**, 2053.

43 (a) M. Finn, R. Friedline, N. K. Suleman, C. J. Wohl, J. M. Tanko, *J. Am. Chem. Soc*. 2004, **126**, 7578. (b) H. S. Taylor, J. O. Smith, Jr. *J. Chem. Phys*. 1940, **8**, 543.

44 K. Hemelsoet, D. Moran, V. V. Speybroeck, M. Waroquier, L. Radom, *J. Phys. Chem. A* 2006, **110**, 8942; and references therein.

45 The TS for the O–O bond cleavage leading to *tert*-butoxy radical is optimized by using 'GUESS=(INDO,MIX)' keyword as we could not optimize the TS with default for initial guess orbital sequence for the trial wave function. The TS involving Pd assisted homolytic O–O bond cleavage could not be located.

46 Methylation in the absence of Pd catalyst has also been studied. See Figs S5-S6 in ESI for additional details.

47 See Fig. S1 in ESI for more details.

48 The Gibbs free energy for generation of methyl radical in the absence of Pd-catalyst is high. See Figs S5-S6 in ESI for energies and TS geometry.

49 The different likely conformers of **TS(B-K)** is examined to ensure that there are no lower energy TSs for **TS(B-K)** than **TS(B-C)**, see Fig. S1 in ESI.

50 Although TS for this step could not be located, we expect that the activation barrier to be low as the activation barrier for a closely related **TS(H-I)** is as low as 1.5 kcal/mol. See Fig. S4 and Table S2 in ESI.

51 (a) The **TS(o-p)** is also optimized in triplet state. The activation barrier is found to be higher.

52 (a) The TS for methyl radical addition at the *meta* and *para*-carbon is also considered. See Fig. S2 in ESI for energetic details. (b) Similarly, a direct C–H activation in intermediate **B**, leading to **K** through **TS(B-K)** is also of higher energy.

53 Singlet diradical TS could not be located and hence the hydrogen abstraction TS is considered only in the triplet state.

54 An alternative pathway involving addition of *tert*-butoxy radical to Pd after the C-H activation is also considered. See Scheme S1, Figs S1, S4,S21 and Table S2 in ESI for additional details.

55 The formation of **k** is found to be exothermic with respect to separated $PdCl_2$ and *tert*-butyl peroxide ($\Delta H = -44.4$, $\Delta G = -32.9$ kcal/mol).

56 The second order perturbation energy representing $n_O \rightarrow \sigma^*_{Pd-Cl}$ delocalization is found to be about 39 kcal/mol at the mPW1K/LANL2DZ, 6-311+G** level of theory. See Fig. S12 in ESI for $n_O \rightarrow \sigma^*_{Pd-Cl}$ delocalization.

57 The intermediate **n** is 20.6 kcal/mol enthalpically less stable than **m**. The geometry of **n** suggests vacant coordination site around palladium. See Fig. S16 in the ESI for a space filling representation of intermediates **m-o**.

58 (a) The enthalpy of complexation is –27.3 kcal/mol. (b) The binding of 2-phenylpyridine to the palladium is primarily facilitated by the coordination of the pyridyl nitrogen, as evident from the N–Pd distance of 2.28 Å.

59 The change in the inter-ring dihedral angles between **o′** and **o** are found to be about 93°, see Fig. S15 in ESI for details.

60 Another higher energy isomeric **TS(o-p')** is provided in Fig. S14 in ESI.

61 (a) J. R. Murdoch, *J. Chem. Educ.* 1981, **58**, 32. (b) M. Anand, R. B. Sunoj, *Organometallics*, 2012, **31**, 6466.

62 Intermediate **q** can have different geometric dispositions of its ligands. The **q** is lower in energy than **a** (ΔH= -20.6, ΔG = -7.2 kcal/mol) and **k** (ΔH= -39.1, ΔG= -25.3 kcal/mol). See Fig. S17 in ESI for additional details.

63 The C–H_{aryl} distances in **a** and **q** are respectively 1.10 and 1.08 Å.

64 Depending on the relative dispositions of the ligands, additional transition state geometries with higher energies for this step are located. Only the lowest energy transition state for this step is presented. See Fig. S17 in ESI for isomeric transition state geometries.

65 See Fig. S18 in ESI for isomeric TS with different disposition of ligands.

66 While this aryl C–H activation is comparable to the **a** to **b** transition described in pathway 1, the hydride in the case of hexacoordinate Pd(IV) intermediate **t** remains on palladium. In the tetracoordinate Pd(II) intermediate **b**, the aryl proton combines with a chloride ligand to form HCl.

67 Participation of a palladium hydride as an active species appears less likely in the present reaction over that of a metal alkyl species. A preference for palladium alkyl over an equivalent

palladium hydride was earlier reported. See D. Roy, R. B. Sunoj, *Org. Biomol. Chem.*, 2010, **8**, 1040.

68 (a) For comparison of Giibs free energy profile for different pathways see Figures S20-S21. (b) The energies at 130 °C (403.15 K) has also been calculated. The Gibbs free energies exhibit the same trend as that obtained at 25 °C, See Tables S3-S4 in ESI for additional details.

69 The free energy change by exchange of product with 2-phenylpyridine from catalyst is very small (ΔH= 0.2, ΔG = 1.2 kcal/mol). See Fig. S19 in the ESI.

TOC Graphics

Mechanism of methylation of 2-phenylpyridine